AMMRC TR 79-9

MICROWAVE TECHNIQUES FOR NONDESTRUCTIVE EVALUATION OF CERAMICS--PHASE II

February 1979

SRI INTERNATIONAL
MENLO PARK, CALIFORNIA 94025

Final Report *Contract Number DAAG46-76-C-0048*

Prepared for

ARMY MATERIALS AND MECHANICS RESEARCH CENTER
Watertown, Massachusetts 02172

The findings in this report are not to be construed as an official Department of the Army position, unless so designated by other authorized documents.

Mention of any trade names or manufacturers in this report shall not be construed as advertising nor as an official indorsement or approval of such products or companies by the United States Government.

DISPOSITION INSTRUCTIONS

Destroy this report when it is no longer needed.
Do not return it to the originator.

SECURITY CLASSIFICATION OF THIS PAGE (When Data Entered)

REPORT DOCUMENTATION PAGE

READ INSTRUCTIONS BEFORE COMPLETING FORM

1. REPORT NUMBER: AMMRC TR 79-9

2. GOVT ACCESSION NO.:

3. RECIPIENT'S CATALOG NUMBER:

4. TITLE (and Subtitle): MICROWAVE TECHNIQUES FOR NONDESTRUCTIVE EVALUATION OF CERAMICS--PHASE II

5. TYPE OF REPORT & PERIOD COVERED: Final Report Covering the Period 30 June 1976 to 9 December 78

6. PERFORMING ORG. REPORT NUMBER: Final Report SRI Project 5594

7. AUTHOR(s): Alfred J. Bahr

8. CONTRACT OR GRANT NUMBER(s): DAAG46-76-C-0048

9. PERFORMING ORGANIZATION NAME AND ADDRESS: SRI International, Menlo Park, California 94025

10. PROGRAM ELEMENT, PROJECT, TASK AREA & WORK UNIT NUMBERS: D/A Proj: M766350; AMCMS Code: 5397-0M-6350

11. CONTROLLING OFFICE NAME AND ADDRESS: Army Materials and Mechanics Research Center, Watertown, Massachusetts 02172

12. REPORT DATE: February 1979

13. NO. OF PAGES: 90

14. MONITORING AGENCY NAME & ADDRESS (if diff. from Controlling Office):

15. SECURITY CLASS. (of this report): Unclassified

15a. DECLASSIFICATION/DOWNGRADING SCHEDULE: N/A

16. DISTRIBUTION STATEMENT (of this report)

Approved for public release; distribution unlimited.

17. DISTRIBUTION STATEMENT (of the abstract entered in Block 20, if different from report)

18. SUPPLEMENTARY NOTES

This project has been accomplished as part of the U.S. Army Materials Testing Technology Program, which has for its objective the timely establishment of testing techniques procedures or prototype equipment (in mechanical, chemical, or nondestructive testing) to insure efficient inspection methods for materiel/material procured or maintained by DARCOM.

19. KEY WORDS (Continue on reverse side if necessary and identify by block number)

Nondestructive evaluation
Microwaves
Silicon nitride
Ceramics

20. ABSTRACT (Continue on reverse side if necessary and identify by block number)

The ability of microwave energy to penetrate some kinds of ceramic materials at frequencies of 100 GHz and higher suggests that microwave techniques may be useful for the nondestructive evaluation (NDE) of such materials. The work described in this report demonstrates the basic feasibility of these techniques for detecting and locating various types of inclusions (including voids) in seeded plates of Si_3N_4. Inclusions as small as 0.005 inch in diameter have been detected using frequencies near 100 GHz.

(continued)

DD FORM 1 JAN 73 1473
EDITION OF 1 NOV 65 IS OBSOLETE

19. KEY WORDS (Continued)

20 ABSTRACT (Continued)

Microwave cross-polarized C-scan images of inclusions have been obtained with a resolution of about one wavelength (3 mm). Some of these images exhibit distinguishing features for different types of flaws.

Various practical aspects that affect the ultimate utility of microwave NDE for ceramics are also discussed.

PREFACE

This report has been prepared under Department of the Army Project Number M766350, Materials Testing Technology. The work reported was performed under Contract No. DAAG46-76-C-0048 for the Army Materials and Mechanics Research Center, Watertown, Massachusetts 02172. Mr. C. H. Hastings served as the Principal Technologist and contract monitor for the Army.

This program has benefited greatly from ideas contributed by the following people at SRI: Dr. U. Gysel, Dr. T. Itoh, Dr. D. Rowcliffe, and Mr. L. Robinson. In addition, the experimental apparatus was constructed and the data obtained by Mr. J. Watjen, Mr. P. Evans, Mr. R. Wanner, Mr. G. Tomlin, and Mr. J. Petro. Particular thanks are also due to Mr. L. Feinstein, a consultant to SRI, who stimulated our interest in this area. Finally, we thank Mr. J. Schuldies of AiResearch Manufacturing Company and Dr. A. Evans of Rockwell International for the loan of several samples of Si_3N_4.

CONTENTS

ILLUSTRATIONS

TABLES

CONVERSION TABLE

1.0 inch = 25.4 mm

1.0 inch = 2.54 cm

0.001 inch = 25.4 μm

I INTRODUCTION

In recent years a great deal of effort has gone into the development of ceramic materials for high-temperature components such as those needed in gas turbines and heat exchangers. Some examples of such materials are silicon nitride (Si_3N_4), silicon carbide (SiC), and lithium-aluminum silicate. Such ceramics are brittle, and their strength is highly dependent on the degree to which defects are present in the material. Because it is impossible to completely eliminate defects, the economic feasibility of using these materials will depend on the availability of nondestructive evaluation (NDE) techniques for locating defects and determining whether they can be tolerated.

A number of different types of defects can occur in ceramic materials. Beside voids, cracks, and density laminations, there can be inclusions of various materials such as tungsten carbide, iron, tungsten, silicon, and carbon. A flaw size of 100 to 200 μm is considered to be critical at room temperature. However, at 1400°C the critical dimension falls in the range 10 to 100 μm for some applications.[1]* The detection of such small flaws represents a severe challenge for any NDE technique, especially since the grain size in high-density hot-pressed material can be as large as 5 μm, and as large as 100 μm in cold-formed material. In addition, the criticality of a flaw depends on its type and geometry. Thus a good NDE technique should also be capable of classifying flaws and providing quantitative information about their size and shape.

A number of different NDE techniques have been evaluated for use with ceramic materials, particularly silicon nitride.[2,3] These techniques include the use of penetrating radiation (X-radiography), penetrating particles (neutron radiography), dye penetrants (both fluorescent and for

---

*References are listed at the end of this report.

enhancing X-radiography), optical radiation (holographic interferometry), and acoustic radiation (conventional ultrasonic inspection, acoustic emission, and acoustic microscopy). Of these, X-radiography and ultrasonic inspection have probably received the most attention.

To achieve the quality of NDE desirable for structural ceramics, it appears either conventional NDE techniques which have been developed for the inspection of metallic components must be significantly improved, or new techniques must be developed. In the area of improved techniques, promising results have been obtained using microfocused X-rays and very-high-frequency (VHF) ultrasonics.[1] However, these techniques are not without their problems. For example, X-radiography is not sensitive to some important flaws such as silicon inclusions, and it is expensive and time-consuming. In the case of VHF ultrasonics, great care must be taken in coupling the ultrasonic transducer to the ceramic. This requirement makes it difficult to move the transducer or sample for scanning purposes and may limit application of the technique to samples with simple geometries.

These limitations indicate a need to explore the possibility of developing other NDE techniques to complement the X-ray and ultrasonic techniques already in use. One possible candidate for a complementary technique is the use of electromagnetic waves at microwave* frequencies, which, for short, are called microwaves. Three main reasons for considering microwaves for this application are

(1) Microwaves can penetrate low-loss dielectric materials, and will interact with local variations in the dielectric properties of these materials.

(2) Microwave transducers (antennas) neither need to be in physical contact with the material to be inspected nor require a coupling medium other than air. Thus, scanning rates will be limited primarily by mechanical considerations.

(3) Microwave technology is well-advanced.

In addition, microwave scattering might provide information about flaws that is not obtainable using other NDE techniques.

---

*The term "microwave" is used here to signify frequencies that are greater than 10^9 Hz (1 gigahertz, abbreviated GHz), and less than 3×10^{11} Hz.

The application of microwaves to various NDE problems has been discussed and studied extensively during the last 15 years.[4-6] Microwaves have been used to probe dielectric materials to measure changes in thickness and material composition, and to detect and locate interior flaws such as voids and inclusions. In ceramic components, the finding and characterization of flaws is of most interest, although a need also exists for quality control in material processing. In the past, the use of microwaves to detect small flaws has suffered from the limited sensitivity and resolution that are dictated by the relatively long wavelengths involved. However, this situation has been improved in recent years by the development of microwave components for use at frequencies up to 100 GHz and beyond. The wavelength in a typical ceramic material at these frequencies is about 1 mm, which is beginning to approach the flaw dimensions of interest. Hence, it appears worthwhile to take a fresh look at microwave NDE for ceramics. The results of such a study are described in this report.

The overall objectives of this work have been to determine the best microwave technique or techniques for the NDE of ceramic components and to define the capabilities and limitations of any such technique. Section II presents a discussion of the various factors involved in selecting a microwave technique for the NDE of ceramics. Some limited data on the dielectric properties of Si_3N_4 at microwave frequencies are presented and discussed in Section III. Section IV describes the experimental systems that were used in the study and gives the results of measurements on seeded Si_3N_4 plates. Then, some practical aspects of microwave NDE that affect its ultimate utility for ceramics are discussed in Section V. Finally, Section VI summarizes the conclusions and recommendations resulting from this work.

II CONSIDERATIONS IN THE SELECTION OF A MICROWAVE NDE TECHNIQUE FOR CERAMICS

A. General

Microwave nondestructive evaluation techniques can be applied to dielectric materials to measure either gross material and geometrical properties (e.g., dielectric constant, dissipation factor, or plate thickness) or localized properties associated with defects.[6] In the evaluation of ceramic materials such as Si_3N_4, one is primarily concerned with the detection of small defects. In this case, the basic physical phenomenon on which the detection is based is the scattering of electromagnetic waves. The two basic characteristics of the scattered wave that can be measured are amplitude and phase (or delay). These quantities can be measured separately or in combination (as in imaging).

For detection of an interior flaw to be possible, the microwave energy must be able to both enter and leave the ceramic material. First of all, this requirement means that the propagation loss inside the material must not be too large. Secondly, the microwave energy must neither be totally reflected from the surface of the material, nor must it be trapped inside the material. The theory for the reflection of a plane wave at an air-to-dielectric interface[7] indicates that some energy will always enter the dielectric material except at grazing incidence. This result is illustrated in Figure 1. The fraction of incident power that is reflected is plotted as a function of the angle of incidence. It is assumed that the relative dielectric constant of the dielectric material is 7, which is typical for Si_3N_4. The figure shows that for other than normal or grazing incidence, the fraction of incident power reflected depends on whether the incident wave has its electric-field vector polarized parallel to the plane of incidence or perpendicular to it. Hence, if a linearly polarized incident wave has its electric-field vector at an angle to the plane of incidence, and if the angle of incidence is between 0° and 90°, the polarization direction of the reflected

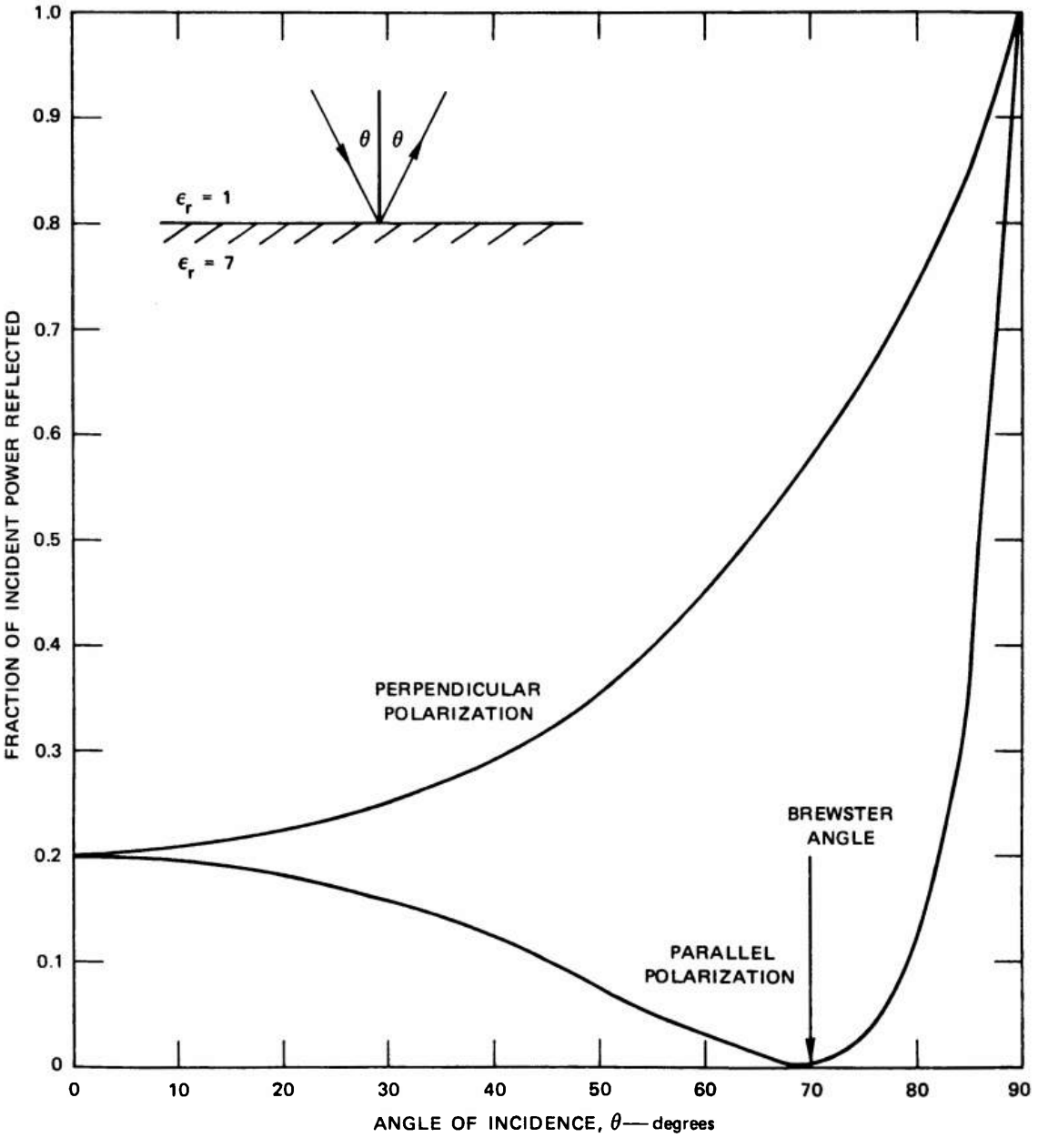

FIGURE 1 REFLECTION AT AN AIR-TO-DIELECTRIC INTERFACE

wave will be rotated.* For parallel polarization there is an angle of incidence where the reflected wave is zero (this angle is called the Brewster angle). Use of the Brewster angle will maximize the transmission of energy through a plane, parallel-sided dielectric plate. However, it is often simplest in practice to choose normal incidence. In this case Figure 1 shows that about 20% of the incident power will be reflected.

After the microwave energy has entered the dielectric material, it will propagate through the material until it meets a defect or a dielectric-to-air interface. Both perturbed and unperturbed waves will usually be partially reflected and partially transmitted when they reach a dielectric-to-air interface. A major exception to this rule, however, occurs when the angle of incidence of the wave at the interface exceeds a certain critical angle. In this case the wave is totally reflected and may become trapped in the material (similar to the way a wave is trapped in a waveguide). This condition can occur if the defect scatters energy over a wide range of angles, or if the geometry of the dielectric-to-air interface varies appropriately.

The behavior of the reflection of a plane wave at a plane dielectric-to-air interface is illustrated in Figure 2. The relative dielectric constants used in computing the curves are the same as those used in Figure 1. The critical angle--about 22°--is fairly small in this case. Hence it is likely that some scattered energy would be trapped in a plate made of such a material.

Because some reflection always exists at a dielectric-to-air interface (except under Brewster conditions), in general there will be standing waves inside the dielectric material. These standing waves will be particularly enhanced if the dielectric specimen is a plate with plane, parallel sides. The presence of standing waves will have a strong effect on the scattering from a defect. For example, suppose the defect were

---

*Also, the reflected wave will be elliptically polarized, but this fact is of secondary importance in the present discussion.

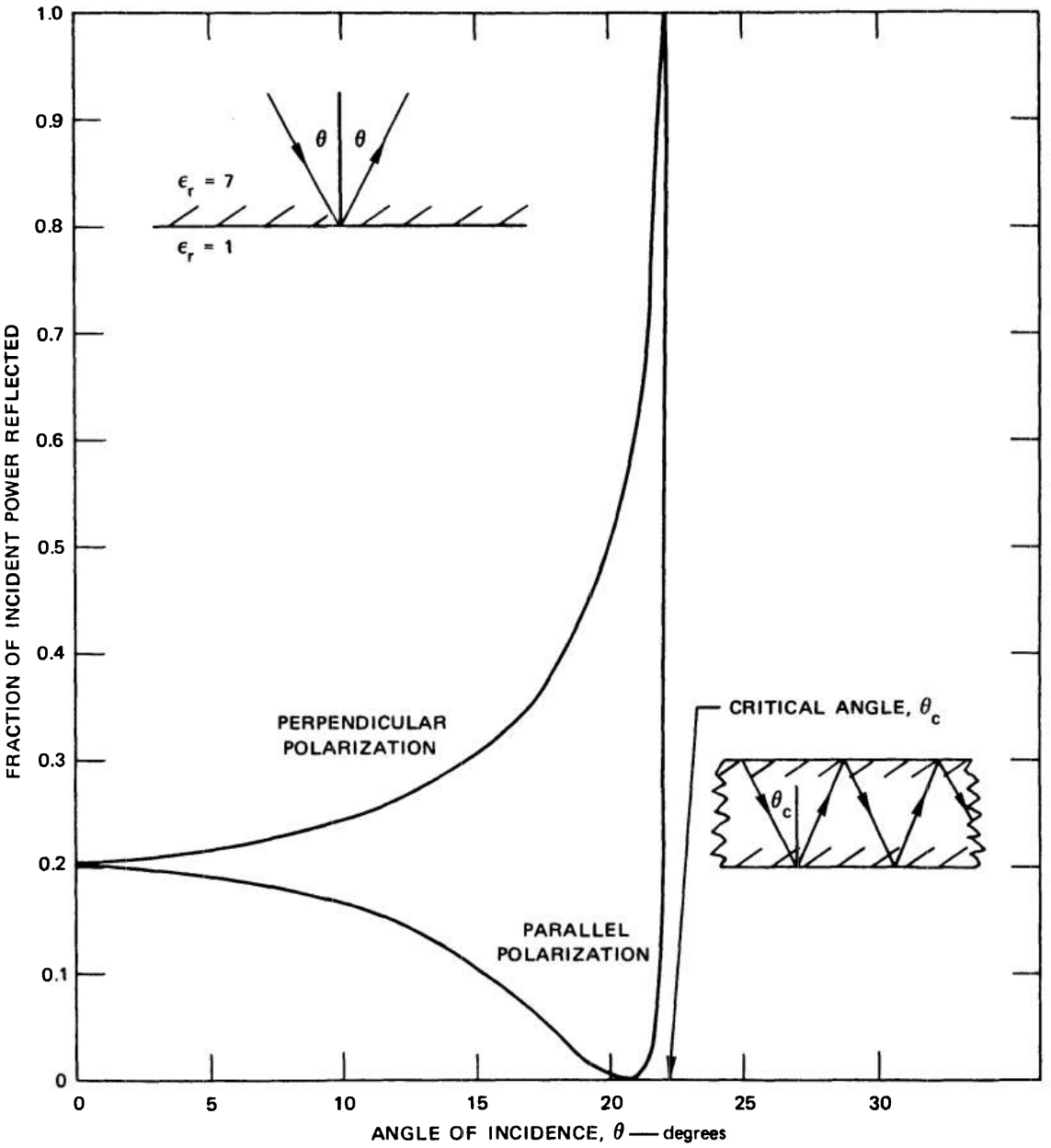

FIGURE 2 REFLECTION AT A DIELECTRIC-TO-AIR INTERFACE

one that only interacts with an electric field. If the defect were located where the electric field in the standing wave is minimum, the scattering would be much less than if the defect were located at a position of maximum electric field. Hence, because the positions of the maxima and minima in a standing wave vary with frequency, the scattering from a defect will exhibit a related frequency variation that will depend on the position of the defect relative to the boundary surfaces of the specimen.

Scattering measurements are usually classified according to the arrangement of the transmitting and receiving antennas and according to the operating frequency. There are three basic antenna arrangements: backscatter-monostatic, backscatter-bistatic, and forward-scatter-bistatic. These three arrangements are illustrated schematically in Figure 3. In the second and third of these arrangements the transmitting and receiving antennas can be either copolarized or cross-polarized, or intermediately polarized.

The horns depicted in Figure 3 represent any kind of appropriate antenna (transducer). Microwave antennas for NDE applications can be characterized as either predominantly radiating or predominantly non-radiating. An example of the radiating type would be a horn or open-ended waveguide. A small aperture in the side of a waveguide or resonant cavity is an example of a sensor that radiates very little. In this case a defect must be close to the aperture so that interaction can take place between the defect and the reactive near fields around the aperture.

B. Sensitivity

In microwave NDE (as in ultrasonics), sensitivity (the ability to detect a defect) depends mainly on two factors: (1) the amount of scattering engendered by the defect, and (2) the ability of the detection technique to separate the desired from the undesired scattered waves. Regarding the second factor, one always strives for high contrast and low background clutter. Electronic noise, a third factor in determining sensitivity, is usually less important than clutter, particularly in a continuous-wave (CW) system.

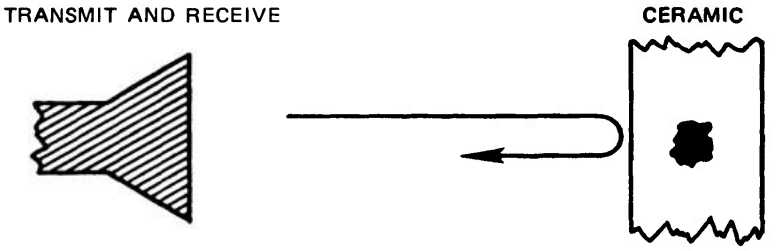

(a) MONOSTATIC BACKSCATTER

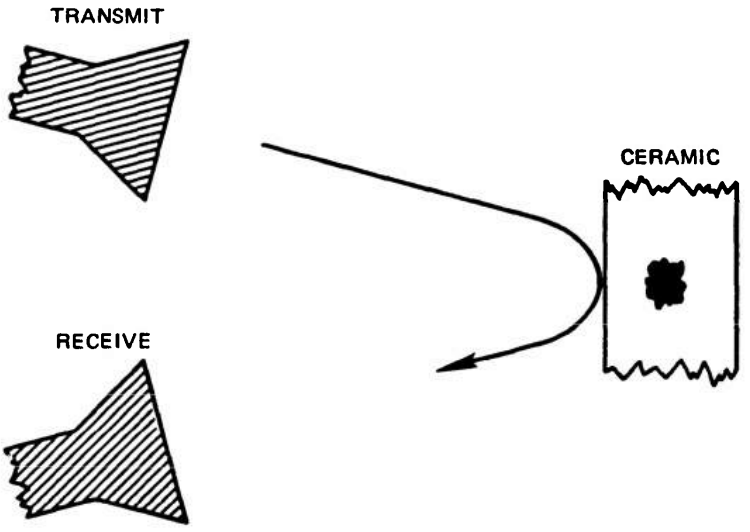

(b) BISTATIC BACKSCATTER

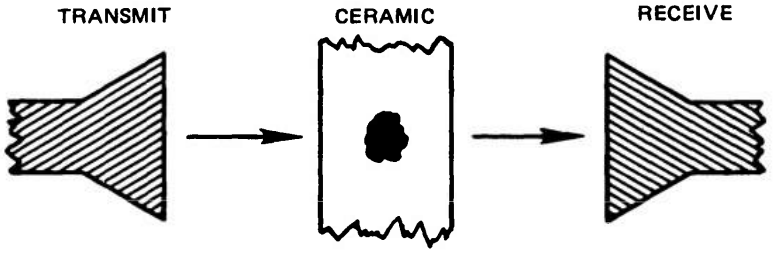

(c) BISTATIC FORWARD-SCATTER

FIGURE 3 SCATTERING CONFIGURATIONS

In general, the theoretical determination of the scattering from an arbitrary shape and type of defect is a difficult problem requiring computer analysis.[8] However, if it is assumed that the defects can be approximated as either metal or dielectric spheres, some rather simple formulas can be used when the wavelength of the electromagnetic radiation is much larger than the sphere radius (Rayleigh region). The Rayleigh criterion is

$$\frac{2\pi a}{\lambda} < 0.4 \tag{1}$$

where λ is the wavelength in the dielectric medium and a is the radius of the sphere. For example, assume that the frequency is 100 GHz and that the dielectric constant of the ceramic is 7.5 (Si_3N_4). Then, from Eq. (1),

$$a < 70\ \mu m \tag{2}$$

in the Rayleigh region.

For a conducting sphere in the Rayleigh region the far-field scattering cross section, σ, for a plane-wave illumination is given by

$$\frac{\sigma(0)}{\lambda^2} = \frac{9}{4\pi}\left(\frac{2\pi a}{\lambda}\right)^6 \tag{3}$$

for backscattering, and by

$$\frac{\sigma(\pi)}{\lambda^2} = \frac{1}{4\pi}\left(\frac{2\pi a}{\lambda}\right)^6 \tag{4}$$

for forward scattering. It can be seen from Eqs. (3) and (4) that backscattering is about an order of magnitude stronger than forward scattering. The quantity σ/λ^2 can be interpreted as the fraction of the total incident power that would be scattered if the total incident power were confined to an area of λ^2.

An expression similar to Eqs. (3) and (4) describes the backscattering from a low-loss dielectric sphere in the Rayleigh region:[9]

$$\frac{\sigma(0)}{\lambda^2} = \frac{1}{\pi}\left(\frac{\varepsilon_r - 1}{\varepsilon_r + 2}\right)^2\left(\frac{2\pi a}{\lambda}\right)^6 \tag{5}$$

where ε_r is the dielectric constant of the sphere relative to the surrounding medium. For example, for a spherical void in Si_3N_4, $\varepsilon_r = 1/7.5$. This value of ε_r makes the factor $[(\varepsilon_r - 1/(\varepsilon_r + 2)]^2$ in Eq. (5) equal to 0.47. Hence such a void should produce Rayleigh backscattering about an order of magnitude smaller than that produced by a metallic sphere of the same radius.

The defects of most interest in the NDE of ceramics have maximum dimensions between 10 and 100 μm. Equation (2) shows that scattering from such defects in Si_3N_4 is of the Rayleigh type even for a frequency of 100 GHz. For this frequency Eq. (3) shows that $\sigma(0)/\lambda^2$ for a metallic sphere ranges between 4×10^{-10} at a radius of 5 μm and 4×10^{-4} for a radius of 50 μm. If the microwave beam is focused to a diffraction-limited spot at the defect so that beam-spreading losses are minor, one can immediately say that the received back-scattered power for these sizes of metallic spheres will be about 100 to 40 dB below the transmitted power. Hence, for these spheres to be detected the clutter (transmit-receive isolation) and receiver noise must be about 110 to 50 dB below the transmitted power level. Clutter rejection of this magnitude is difficult to obtain in practice, and so users of microwave techniques may face difficulties in attempting to detect such small defects.

The above calculations give one a rough feeling for the sensitivity required, but they may be considerably in error because (1) defects are not usually spherical, (2) near-field rather than far-field sensing may be used, and (3) it is often advantageous for purposes of clutter rejection to detect the orthogonally polarized scattering from the presumably assymetrical defect, for which the mode-conversion efficiency is unknown. Hence, an experimental evaluation of each candidate microwave technique for various types of defects is required.

If the defect is larger than that considered above, or if the frequency is higher, interference between the scattering from different parts of the defect can occur. In this situation--called resonance scattering--increases in scattering cross section of 1 to 2 orders of magnitude over that existing at the upper end of the Rayleigh region are

often observed. Hence, operation at frequencies higher than 100 GHz may prove advantageous if the scattering from surface irregularities and grain boundaries is not too large.

C. Clutter Rejection

Obtaining adequate clutter rejection is of major importance in microwave NDE. In conventional radars and ultrasonic NDE systems, clutter can be rejected by pulsing the interrogating signal on and off and gating out the desired return signal in the time domain (called range gating). Alternatively, the clutter detected by a CW coherent radar can be rejected by Doppler processing when there is relative motion along the direction of propagation between the radar and the target (but not the background). Neither of these techniques is applicable in the microwave NDE of ceramics.

The use of pulsed measurements (or, equivalently, wideband swept-frequency measurements) for range gating is not advantageous in microwave NDE because most ceramic components are relatively thin (a few wavelengths thick or less), and the shortest practical pulse that can be produced and radiated results in a spatial extent for the pulse that is typically of the order of 10 wavelengths or more in the ceramic material. Thus, reflections from boundary surfaces and defects tend to overlap in the time domain.

As for Doppler processing, moving the part being inspected along the direction of propagation also moves both the clutter-producing boundary surfaces and the defect, thereby imparting the same Doppler shift to the reflections from both types of scatterer. Hence, Doppler processing cannot separate the desired signal from boundary scattering.

However, another contribution to clutter exists, namely, direct leakage between the transmitting and receiving systems. Moving or vibrating the part being inspected will permit rejection of this clutter component because the direct leakage is not modulated by the moving target.[10]

One other possibility exists for modulating the return from a defect without producing commensurate modulation of the clutter: vibrating or rotating the target transversely to the direction of propagation (or, equivalently, scanning the beam back and forth slightly in a transverse direction). The transverse excursion should be on the order of a wavelength. If the spatial extent of the microwave beam is sharply defined, the scattering from a highly localized defect will be modulated as the vibrating defect passes through the beam. If one assumes the boundary surfaces in the neighborhood of the defect are smooth and flat compared with a wavelength, the modulation of the clutter produced by these boundary surfaces should be considerably less than the modulation of the defect-related signal. Thus, the desired signal can be separated from the clutter by filtering.

All of the clutter-rejection techniques discussed so far operate on the received signal in either the time or frequency domains. It should also be possible in some instances to reject clutter by spatial filtering. For example, if the horns shown in Figure 3(b) are focused, they can be arranged so that very little of the energy specularly reflected from the sample enters the receiving antenna, if one assumes no sharp geometrical discontinuities (other than flaws) lie in the path of the illuminating beam. Of course, the bistatic scattering properties of the flaw must be such that the flaw <u>will</u> scatter energy into the receiving antenna.

Two other approaches to clutter rejection involve the use of bridge techniques and/or mode conversion.[11,12] One simple type of bridge is one in which a portion of the transmitted signal with the proper amplitude and phase is fed directly to the receiver so that the signal received in the absence of a defect is canceled. This type of arrangement is called a feed-forward canceller. Another type of bridge is a phase bridge that can be implemented using a homodyne receiver. Here, the clutter can be canceled by adjusting only the phase of a reference signal. The problem with these techniques is that the bridge balance is sensitive to the positions of the specular scatterers that produce the clutter, and thus it is difficult to keep the bridge balanced as the part being inspected is

scanned (unless the part is a well-aligned flat plate). This variation in bridge balance is one form of "lift-off" effect.*

Even if bridge balance could be maintained, if the clutter signal being canceled is large, a relatively small signal produced by a defect will not be effective in unbalancing the bridge and sensitivity will be reduced. Hence, it is better to minimize the amount of clutter that enters the receiver, while at the same time maximizing the detection of the defect-related signal. This can be done to a certain extent by using mode conversion. For example, a linearly polarized wave imginging perpendicularly on a flat plate will be reflected without converting any energy to the orthogonally polarized mode. On the other hand, an assymmetrical defect will scatter energy into the orthogonal mode. Thus, in this case clutter can be rejected to the extent that the orthogonal linearly polarized modes can be separated in the receiver.

If the material to be inspected is (partially) transparent to microwaves, it is perhaps simplest to implement the mode-conversion technique by utilizing the bistatic forward-scatter system of Figure 3(c) and orienting linearly polarized transmitting and receiving antennas orthogonally to one another. If the material is not transparent, the monostatic backscatter system of Figure 3(a) can be used in conjunction with a so-called orthomode coupler for separating the orthogonal modes.

The sensitivity of a microwave NDE system can be defined as the amplitude of a defect-related signal that is 3 dB larger than the clutter or receiver noise, whichever is larger. Usually, some clutter or background signal which is larger than the noise is left even after rejection by mode conversion. This remaining clutter signal can be reduced further, hopefully to the limit imposed by system noise, by utilizing some form of bridge like those discussed earlier. The balancing of the bridge is now less critical, however, because the clutter signal to be cancelled by the bridge has been reduced by orthogonal mode rejection. Because a

---

*A lift-off effect in electromagnetic NDE refers to any variation in detected signal that is caused by a change in the distance between the sensor and the sample.

sensitivity of 50 to 100 dB below the transmitted power level is likely to be required (see Section II-B), and because the transmit-receive isolation achievable using mode conversion is usually less than this amount, a practical microwave NDE system might require the use of a combination of mode-conversion and bridge techniques.

D. Spatial Resolution

Two basic types of spatial resolution can be defined. One--"global" resolution--is concerned with one's ability to locate a defect relative to some reference location, and the other--"local" resolution--is concerned with one's ability to differentiate between two closely spaced defects.

As discussed previously, for thin ceramic parts microwave NDE does not provide any spatial resolution in the nominal direction of propagation of the illuminating wave. In the scanning plane (defined as a plane containing all the positions of a reference point on the sample that are occupied as the sample undergoes rectilinear translation), spatial resolution is determined by the active areas of the transmitting and receiving antennas. At distances sufficiently far removed from the test piece, the "active" area is essentially determined by the far-field beamwidth of the radiating antenna.

A simple microwave antenna such as a horn must have an aperture that is several wavelengths on a side in order to minimize spreading of the beam. The beamwidths associated with this kind of antenna result in a local spatial resolution in the scanning plane that is much too gross for the ceramics application.*

The best spatial resolution using a far-field antenna is obtained by incorporating a lens into a microwave horn.[13] Such a lens can be

---

*In principle, a "synthetic array" technique could be used to improve resolution along the line of scan. In this technique, the amplitude and phase of the scattered waves received at a number of successive sample points along the scan line are stored and then the data are processed by computer to form a higher resolution image.

fabricated from polystyrene, and produces a 3-dB spot size having a diameter approximately equal to one free-space wavelength at the operating frequency. Focal lengths of such lenses are typically 10 wavelengths. For reference, it is useful to keep in mind that the free-space wavelength at 100 GHz is equal to 3 mm.

An alternative approach to using a lens that can yield comparable magnitudes of resolution, is to move the test piece into the near fields of the antennas. In this case the active area of the antenna is simply equal to the effective aperture of the antenna. The size of this effective aperture depends on the nature of the fringing fields around the aperture and the distance between the aperture plane and the scanning plane.

One of the simplest types of antenna is an open-ended waveguide. Typical aperture dimensions for such an antenna at 100 GHz are about 0.4 by 0.8 free-space wavelengths, or 1.25 by 2.5 mm. Higher resolutions can be obtained by reducing the aperture size[10] (i.e., by using an electrically small antenna and moving closer to the test piece). However, this approach results in a trade-off between sensitivity and resolution. Overall sensitivity is lost when the aperture size is reduced because less of the total available power "leaks" through the aperture (unless there is compensation by appropriate impedance matching). In addition, an electrically small antenna radiates relatively very little energy, and the near fields associated with it fall off very rapidly with distance from the antenna. Thus, with such an antenna, one runs the risk of not detecting a defect inside the ceramic material.

An important advantage of obtaining good local spatial resolution is the minimization of spurious scattering caused by variations in the gross geometry of the ceramic part. Signals caused by slow variations in geometry can be removed by filtering, but a small active sensor-area is the only solution for inspecting a part very close to a sharp change in boundary surface (such as an edge).

III DIELECTRIC PROPERTIES OF Si_3N_4 AT MICROWAVE FREQUENCIES

Detection of flaws within Si_3N_4 depends on the losses in the material being small and the existence of some difference between the dielectric properties of the Si_3N_4 and those of the flaw. Because little information is available on the dielectric properties of bulk Si_3N_4 at high microwave frequencies, SRI conducted experiments to obtain more data.

The dielectric properties of Si_3N_4 depend on the process used for fabrication (reaction sintering, hot pressing, etc.). Published data taken at 10 GHz on samples of Si_3N_4 produced by different processes show values of relative dielectric constant ranging between 5.5 and 9.3, and loss tangents ranging between 0.001 and 0.15.[14] Hence, measurements were conducted during this program using both reaction-sintered and hot-pressed material (Norton NC132), with particular emphasis on the latter material.

Two different measurement techniques were used. For frequencies up to 18 GHz, the reflection and transmission properties of a sample inside a coaxial holder were measured with a Hewlett-Packard Model 8542B automatic network analyzer. For higher frequencies, free-space measurements of the reflection and transmission for a plane, parallel-sided plate were used.

In the automatic-network-analyzer (ANA) system an SRI-generated computer program accepts the measured complex reflection and transmission data and calculates the following material parameters:[15]

- the complex air-material interface E-field reflection and the complex propagation constant within the material that would exist as if the material were semi-infinitely thick with only one air-material interface,
- the complex relative dielectric constant, ε_r (permittivity),

- the complex relative permeability, μ_r,*
- the loss tangent, and
- the attenuation constant of the material, in dB/cm.

The measurement procedure in this case requires that the sample be in the form of an annulus. This sample is mounted in a precision 50-ohm, 7-mm beadless-airline coaxial transmission line (Maury Microwave Model 2653-1250). This holder permits measurements to be made over a very wide frequency range and eliminates the measurement errors associated with the small reflections produced by the dielectric support beads in a conventional coaxial line. The diameter of the outer coaxial conductor of the transmission line is 7.00 mm; the diameter of the inner one is 3.04 mm. The samples that were measured were cut and ground to be a slip fit to the coaxial line by a local ceramics fabrication house (RW Products, Redwood City, California).

The dielectric properties of three different ceramic materials were measured using the ANA system. The first material tested was a piece of reaction-sintered Si_3N_4 obtained from the Materials Center at SRI. The sponsor provided a second sample that was intended to be hot-pressed Si_3N_4 (Norton NC132), but which proved to be hot-pressed silicon carbide (SiC). This fact was determined from X-ray diffraction analysis. Therefore, some Norton NC132 obtained from the SRI Materials Center served as the third test material.

The SiC sample was found to have so much dissipation loss (in fact it exhibited dc conductivity) that the calculated values of ε_r probably have little meaning. The air-material interface reflection was high--about 0.85 at all frequencies from 0.2 GHz to 18 GHz. The attenuation within the material was very high, ranging from about 10 dB/cm at 1 GHz, to about 70 dB/cm at 10 GHz, to about 100 dB/cm at 18 GHz. Thus, microwaves would not be suitable for probing very far into this material.

---

*For Si_3N_4, the permeability was assumed to be the same as for free space. However, the computer program is general enough to handle magnetic materials.

The fraction of reflected incident power and the attenuation for infinitely thick samples of reaction-sintered and hot-pressed Si_3N_4 are plotted as functions of frequency in Figure 4. These results were derived from measurements using a sample of finite thickness. The reaction-sintered material appears to be less dense than the hot-pressed material because the power reflected from the reaction-sintered material is less than that for the hot-pressed material. The corresponding derived values for the real part of the relative dielectric constant are:

- Hot-pressed Si_3N_4: $\varepsilon_r = 7.5$ (at 8.0-17.5 GHz)
- Reaction-sintered Si_3N_4: $\varepsilon_r = 5.7$ (at 8.0 GHz) to 6.0 (at 17.5 GHz).

On the other hand, the attenuation in the reaction-sintered material was higher than for the hot-pressed material. In fact, the losses in the hot-pressed material were so low that the attenuation could not be measured accurately at most of the measurement frequencies. Such low losses cause the data-reduction computer program to give inaccurate results for the dielectric parameters when the sample is an integer multiple of one-half wavelength thick. One can see from Figure 4 that this situation occurs at about 13.5 GHz, where the sample is one wavelength thick (4.06 mm). Fortunately, alternate data reduction of the reflection coefficient and insertion loss of the finite sample provide accurate means for determining the reflection factor and attenuation at this frequency. The resulting calculated value for the attenuation, plotted in Figure 4, is less than 0.2 dB/cm.

It can be concluded that, for frequencies up to 17.5 GHz, the values of reflection factor and attenuation for Si_3N_4 (either type) do not prevent the use of microwave NDE. However, one can anticipate the need to operate at higher microwave frequencies--for example, in the range 50 to 100 GHz--to obtain better sensitivity and resolution. Hence, some measurements were also conducted at these higher frequencies.

One approach for determining the dielectric constant of ceramic materials at frequencies above 50 GHz is based on the fact that the reflection from a plate having flat, parallel faces is a minimum whenever

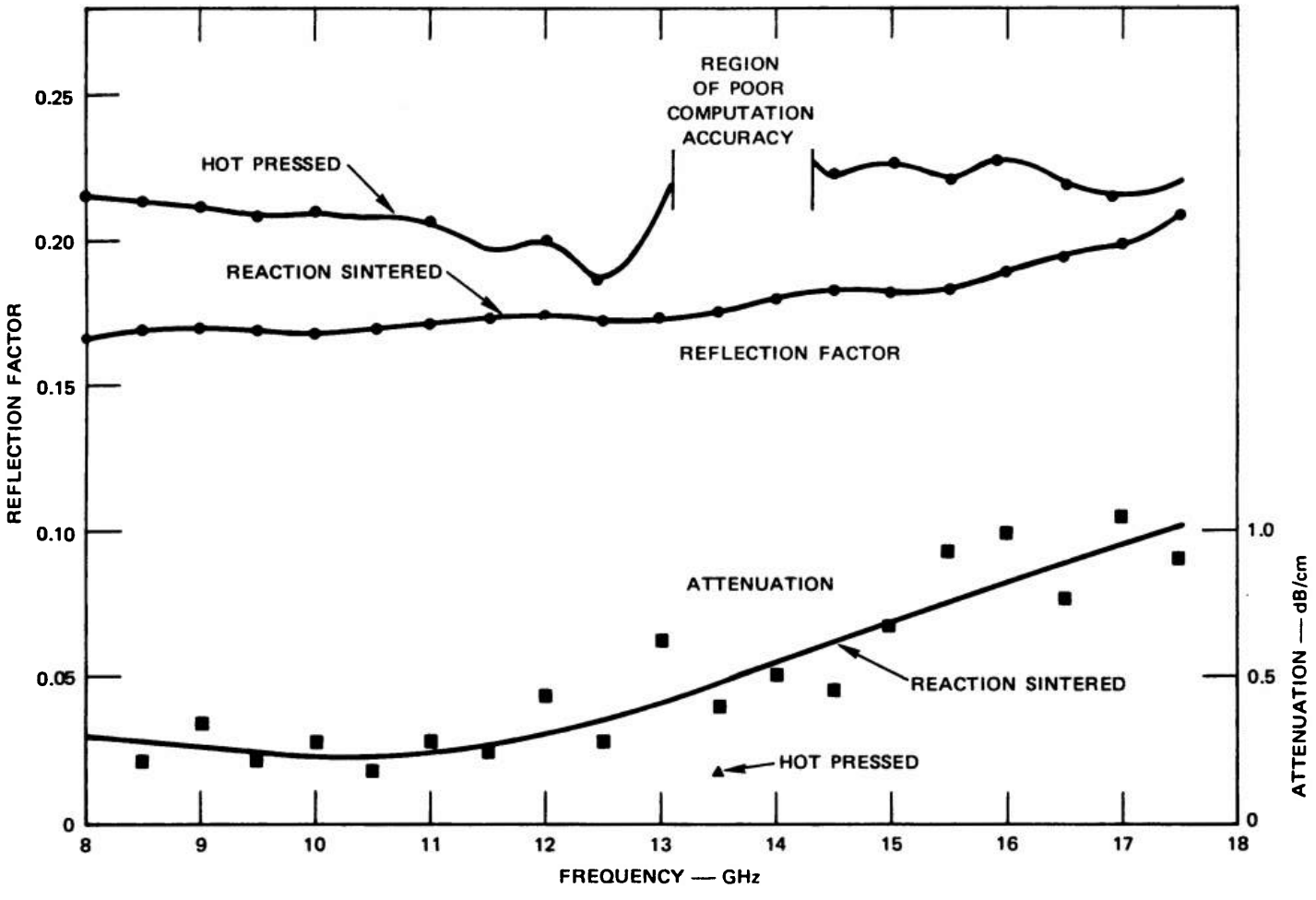

FIGURE 4 MEASURED DIELECTRIC PROPERTIES FOR Si_3N_4

the thickness of the plate is an integer multiple of one-half the wavelength in the material. If f_1 and f_2 are adjacent frequencies at which reflection minima occur, the relative dielectric constant, ε_r, can be computed from the equation

$$\varepsilon_r = [c/(f_2 - f_1)2t]^2 \tag{6}$$

where c is the velocity of light in free space and t is the thickness of the plate. For example, for a hot-pressed Si_3N_4 plate 6.35 mm thick, it was found from measurement that f_1 = 53 GHz and f_2 = 62 GHz. Substitution of these numbers into Eq. (6) gives the result ε_r = 6.9. This value is comparable to, but smaller than, that obtained at lower frequencies; this discrepancy could be caused by experimental error.

The output power as a function of frequency of the available broadband 100-GHz source (a backward-wave oscillator) was too erratic to permit determination of ε_r at 100 GHz. However, it was possible to measure the average insertion loss of several hot-pressed NC132 Si_3N_4 plates for frequencies between 99 and 101 GHz. This was accomplished by first establishing a reference level for the free-space transmission between two colinear antennas, and then noting the increase in radio frequency (RF) power required to reestablish the reference level after a ceramic plate had been placed between the antennas perpendicular to the beam. The loss measured in this way is the sum of the reflection loss (a function of frequency) and the dissipation loss. The results are shown in Table 1. In evaluating these data note that the maximum possible reflection loss of a plate having ε_r = 7 is 3.6 dB. Hence the dissipation loss in hot-pressed Si_3N_4 at 100 GHz is not large enough to constitute a major limitation for the microwave NDE of this material at this frequency.

Table 1

AVERAGE TRANSMISSION LOSS THROUGH HOT-PRESSED Si_3N_4 (NC132) AT 100 GHz

Billet Number	Thickness (mm)	Average Loss (dB)
E307103897	5.69	3.1
D200974-1158	6.75	2.8
F307104930	6.38	1.0

IV EXPERIMENTAL DETECTION AND LOCATION OF DEFECTS IN Si_3N_4

A. General

Two types of microwave scattering measurements were conducted during this program. One type involved incoherent transmission (forward scatter), and the other involved coherent backscatter. These measurements were performed both in the near field using open-ended-waveguide antennas and in the far field using a lens-focused antenna. Normal incidence was always used. Because the microwave antennas were fixed, scanning was accomplished by moving the sample. Experiments were conducted at frequencies between 10 and 100 GHz; however, most of the experimental data were taken at frequencies near 100 GHz, because the highest frequencies provided the greatest sensitivity and resolution. The following subsections describe the microwave measurement systems that were used, and present the experimental results obtained using seeded plates of Si_3N_4.

B. Microwave NDE Measurement Systems

Block diagrams of the microwave systems used in this program to measure the scattering from flaws in ceramics are shown in Figure 5. Figure 5(a) shows the simpler of the two systems, namely a transmission measurement system. The antennas in this system were aligned along a vertical axis and cross-polarized. When the creamic sample to be inspected was a flat plate with parallel faces aligned perpendicularly to the antenna boresight axis, a transmit-receive isolation in excess of 45 dB could be achieved by adjusting the polarization of the receiving antenna with respect to that of the transmitting antenna. Video detection was used for convenience, since it is physically difficult to interconnect the waveguides that would be required to implement a coherent transmission system. In this system the transmit-receive isolation was large enough so that the sensitivity was determined by the electronic

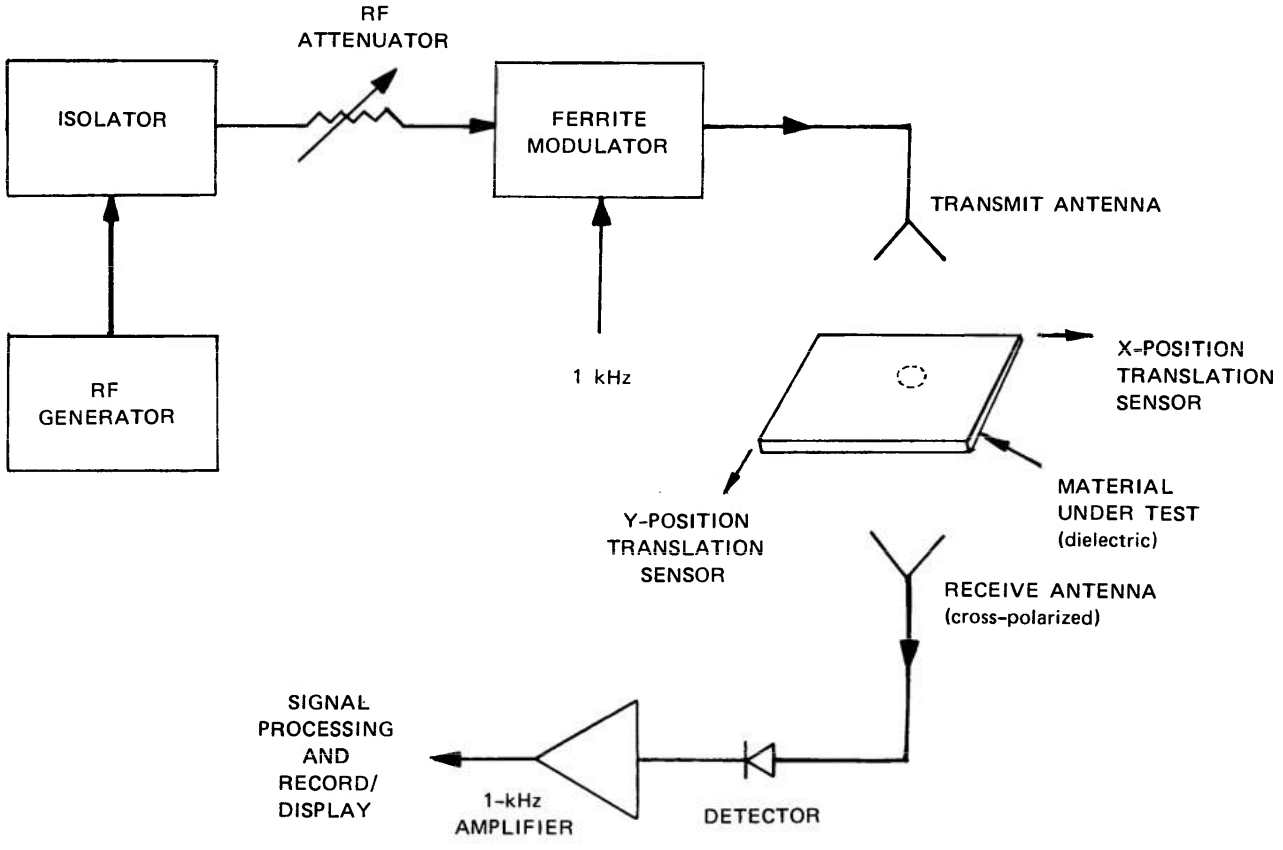

(a) SYSTEM FOR MEASURING CROSS-POLARIZED TRANSMISSION USING VIDEO DETECTION (incoherent)

FIGURE 5 MICROWAVE SCATTERING-MEASUREMENT SYSTEMS

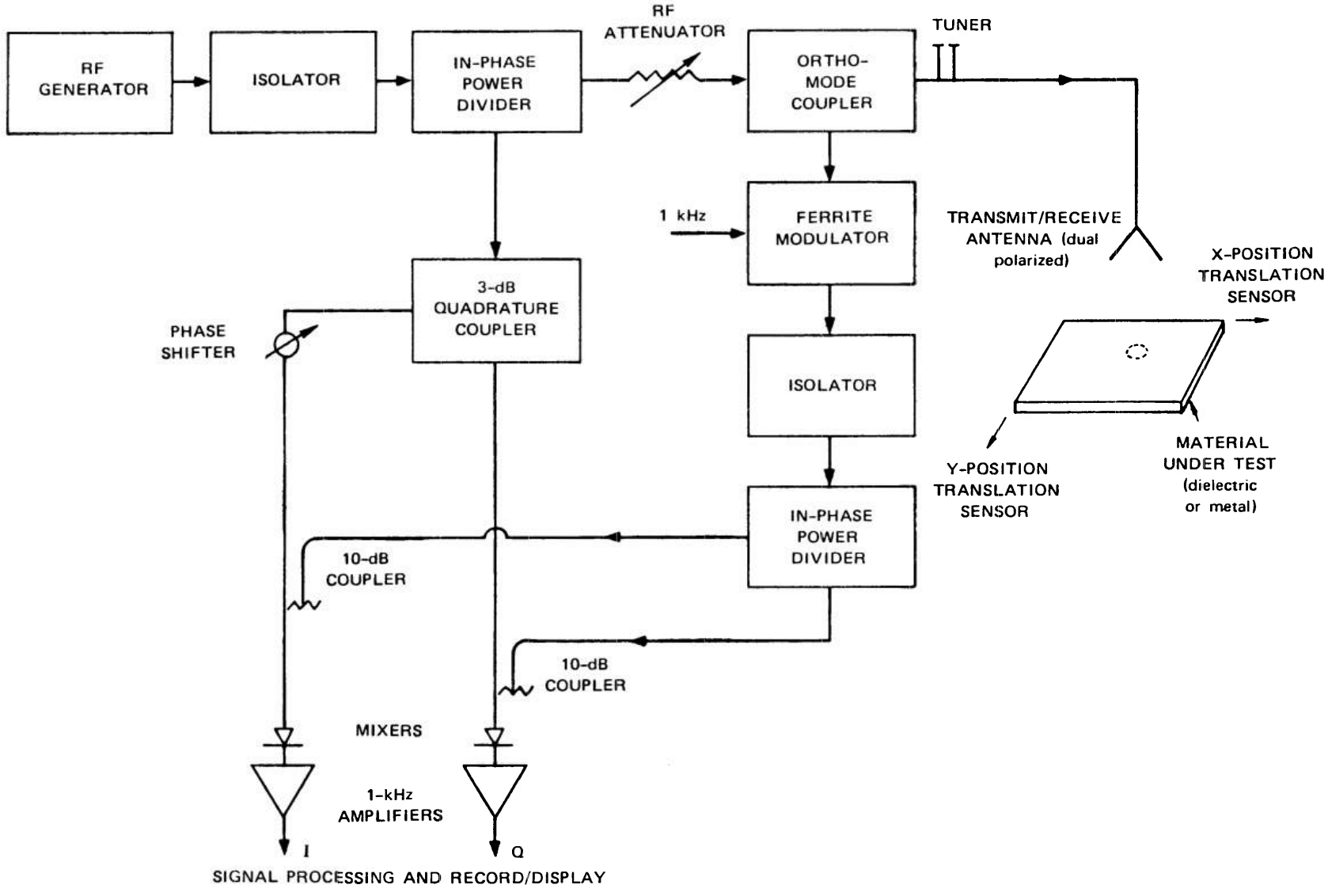

(b) SYSTEM FOR MEASURING CROSS-POLARIZED BACKSCATTER USING HOMODYNE DETECTION (coherent)

FIGURE 5 (Concluded)

noise; the minimum detectable signal power in this case was about -40 dBm.* It appeared that the clutter (leakage) signal in this system was only a few dB below the system noise. Hence, the flaw-detection sensitivity would not be improved very much by increasing the RF signal power. The bandwidth of this type of system is usually determined by the frequency response of the antennas; the broadest achievable bandwidth is a full waveguide band, e.g., 75 to 100 GHz. Additional discussion of such a transmission system can be found in an earlier report.[17]

A block diagram of the other measurement system used during this program--a coherent backscatter system--is shown in Figure 5(b). This system uses a single antenna for both transmitting and receiving; hence, the antenna-alignment complications present in the transmission system are eliminated. The coherent backscatter system is a homodyne system that uses quadrature detection to measure the amplitude and phase of the backscattered signal. If the detected in-phase and quadrature voltages are called I and Q, respectively, the backscatter amplitude is given by $\sqrt{I^2 + Q^2}$, and the phase is given by $-\tan^{-1}(Q/I)$. To obtain accurate I and Q signals the difference in phase lengths between the signal and reference arms for the I channel must be equal to the corresponding difference in phase lengths for the Q channel.

The RF "heart" of this backscatter system is the orthomode coupler that separates the received cross-polarized waves from the undesired co-polarized waves (clutter). The isolation of the particular coupler used in this program (TRG Model W881) was 40 dB at 100 GHz with the copolarized output terminated, and its bandwidth was about 3 percent. However, because of the cross-polarized leakage contributed by the large copolarized wave backscattered from the sample, the actual isolation (clutter rejection) varied between 25 and 55 dB, depending on the frequency and the distance to the sample. By the judicious choice of frequency, the use of tuning screws at the copolarized output of the coupler, and the careful alignment of the sample, it was possible to achieve a clutter level of about -50 dBm. This level was still several

*dBm = decibels referred to a milliwatt.

dB above the noise of the system but represents an improvement in sensitivity over the bistatic video-detection system of about 10 dB. However, it was difficult to maintain this improved sensitivity during inspection because the clutter rejection using the orthomode coupler was very sensitive to drifts in RF frequency and changes in the antenna-to-sample distance. In this situation, reducing the loss in the signal path or increasing the RF generator power would not improve the flaw-detection sensitivity.

The I and Q outputs of this homodyne system are video signals that carry the 1-kHz square-wave modulation that is applied to the transmitted RF signal. These video signals are amplified by narrowband 1-kHz linear amplifiers. These amplifiers are, in fact, HP 415E standing-wave-ratio meters and have a maximum dynamic range of about 15 dB for any particular gain setting. The gains of these amplifiers were usually set so that the clutter level was slightly less than the smallest signal detectable at that gain setting. Signals 15 dB larger than this minimum detectable signal level are clipped, which was of no concern, because the main objective was to detect the smallest flaws possible.

A photograph of an open-ended-waveguide antenna is shown in Figure 6. The waveguide was milled in a split aluminum block that is 1.125 inches on a side. The waveguide protrudes 0.1 inch above the surface of the block--the area surrounding the protruding waveguide is covered with lossy material to minimize multiple reflections between the antenna and the sample. A detector is connected directly to the other end of the block.

The inside dimensions of a waveguide suitable for 100 GHz are 0.050 by 0.100 inch (1.27 by 2.54 mm) or 0.42 by 0.84 wavelengths. This type of antenna produced the best local spatial resolution when it was placed as close as possible to the surface of the ceramic sample. In this case, the resolution achievable for a surface flaw is approximately equal to the dimensions of the waveguide opening. The resolution becomes poorer if the flaw is located farther from the antenna. For example, if the flaw is located 4 mm from the aperture plane of the open-ended waveguide,

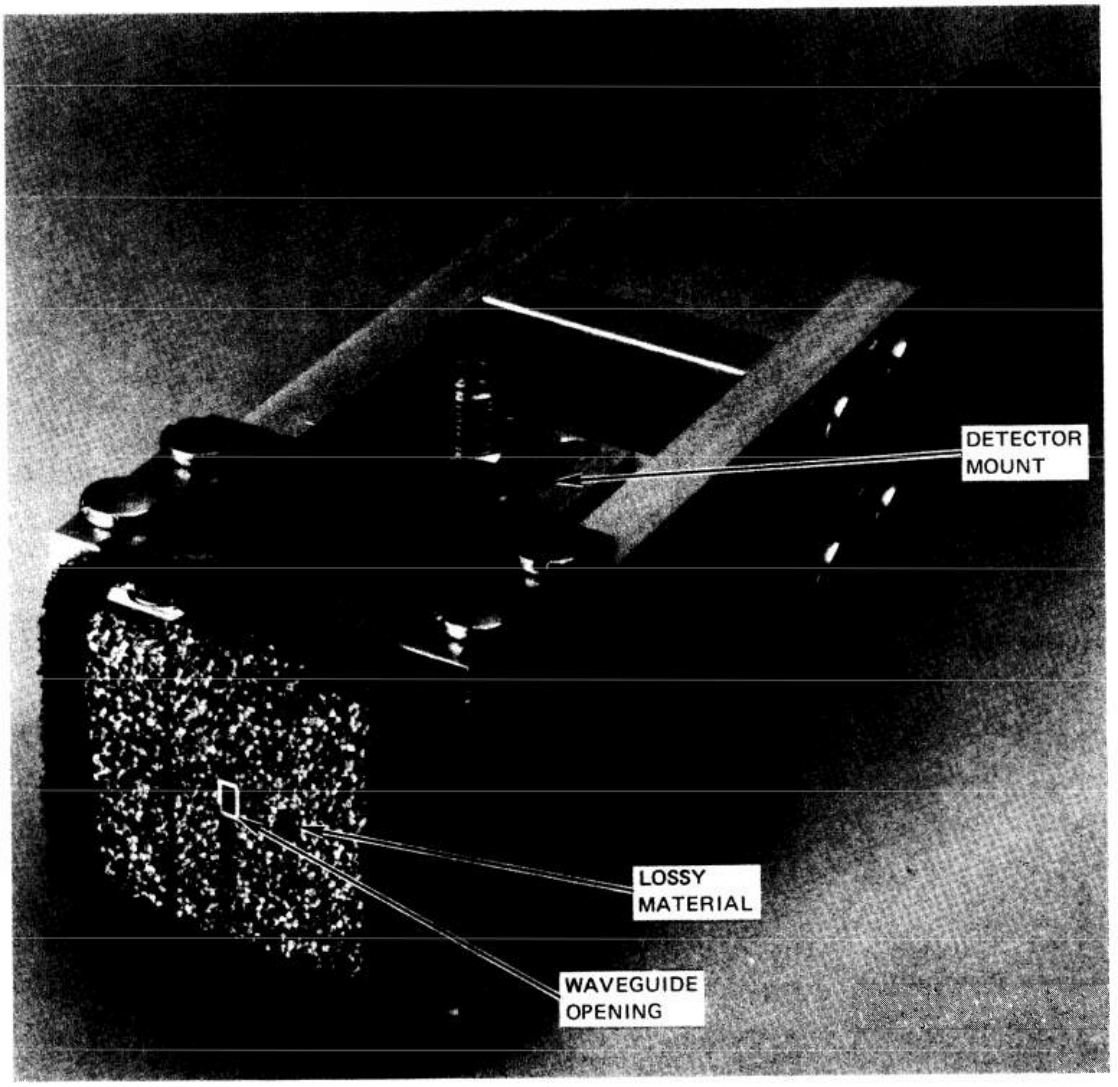

FIGURE 6 OPEN-ENDED WAVEGUIDE ANTENNA

the 3-dB beamwidth[16] at 100 GHz in the plane containing the flaw is about 14 mm in the E plane, and 6 mm in the H plane.* This degree of resolution was adequate for studying the widely spaced defects in the 6-mm-thick seeded plates that were examined during this program.

A photograph of the 100-GHz homodyne backscatter system is shown in Figure 7. The lens-focused antenna used in this program (TRG model W857-3) is indicated in the figure. The lens is 3 inches in diameter and has a focal length of 3 inches. The lens produces a diffraction-limited spot about one wavelength in diameter (3 mm) and has a depth of focus of several wavelengths. The RF source shown in the photograph is an IMPATT diode with an output power of +14 dBm and a mechanical tuning range of 97.5 to 102.5 GHz. A backward-wave oscillator was also used during the program. Its output power was of the same order of magnitude as the IMPATT diode, but it could be electrically tuned over the full waveguide band of 75 to 100 GHz. The microwave hardware is mounted on a 20 by 28-inch board. The size of this support structure was chosen for convenience--the system could be configured much more compactly if desired. The mounting board was supported by three leveling screws that permitted the antenna axis to be aligned vertically.

Because the waveguide hardware could not be moved, the samples were scanned by moving them in a plane transverse to the antenna boresight axis. A mechanical X-Y stage was built for this purpose (a photograph of this stage is shown in Figure 8). The stage frame measures 24 by 36-inches. The stage is driven continuously in the X direction, and the maximum length of travel in that direction is 10 inches. A stepping motor moves the stage in the Y direction with a minimum step size of 0.010 inch and a maximum length of travel of 8 inches. A superstructure mounted to the frame supports the open-ended waveguide receiving antenna when the system is used for making transmission measurements. When this antenna is not in use, it can be slid out of the way to the rear of the frame. The entire frame is supported by four leveling screws.

---

*In antenna parlance, the E-plane is a plane containing the transverse E-field and the direction of propagation. Similarly, the H-plane contains the transverse H-field and the direction of propagation.

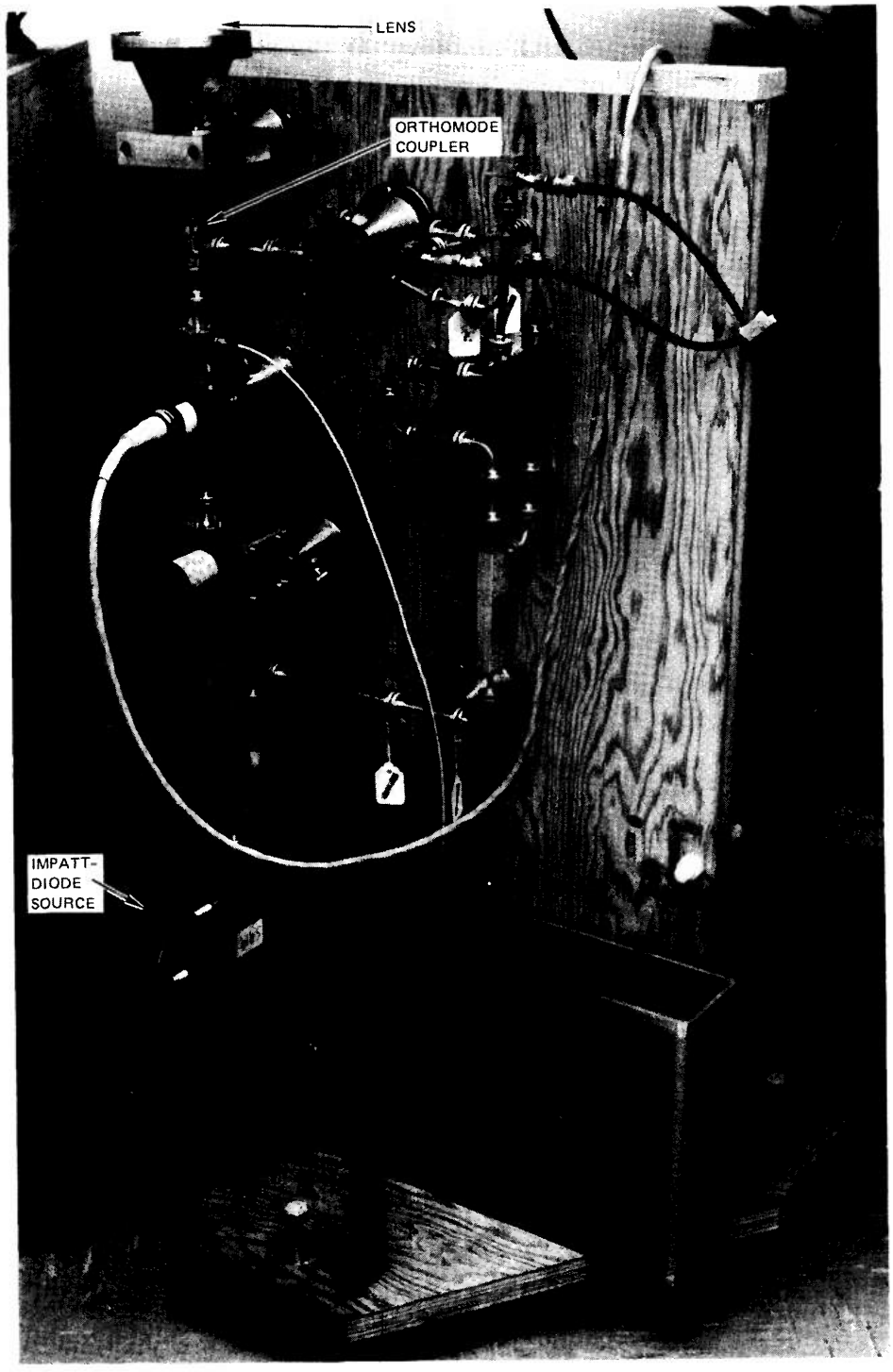

FIGURE 7 100-GHz HOMODYNE BACKSCATTER SYSTEM

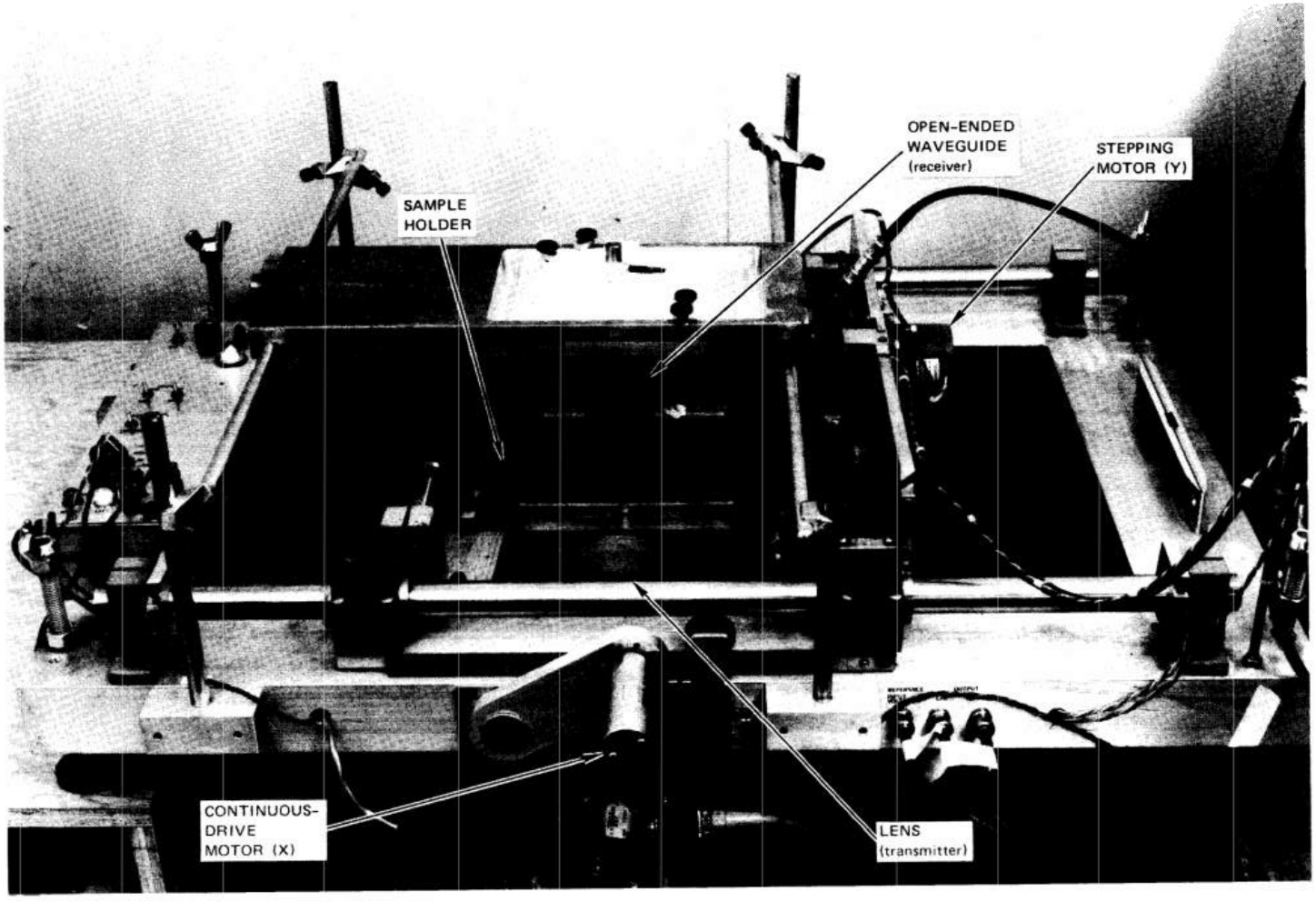

FIGURE 8 MECHANICAL X-Y STAGE

The creation of C-scan images having good resolution over several square inches of area requires the acquisition of a considerable amount of data. To speed up this process, minimize operator error, and improve positioning accuracy, a digital-stage-control and data acquisition system was designed and built. A block diagram of this system is shown in Figure 9. After the pairs of starting and stopping coordinates and the step size in the Y direction are programmed into the system, the controller moves the stage to scan the area defined by these coordinates a line at a time. The I and Q signals are correspondingly sampled, digitized, and stored on cassette tape. This tape is then played back into a minicomputer for subsequent processing and display. In addition, a real-time display of each scan line is generated as data are being acquired. A photograph of the front panel of this system is shown in Figure 10.

C. Experimental Results

The experimental results obtained during this program were for one material: Si_3N_4. The samples that were examined were all in the form of flat plates containing seeded inclusions, and were mostly made from hot-pressed material (NC 132), although one sample of reaction-sintered material was also examined.

Measurements conducted during the first phase of this program were performed with a microwave transmission system that used open-ended waveguides for both transmission and reception [see Figure 5(a)]. These antennas were placed as close as possible to the surfaces of the sample. Preliminary measurements were made in the frequency range 40 to 60 GHz, but it was soon established that frequencies in the neighborhood of 100 GHz provided better sensitivity and resolution. Therefore, all data presented in this report were obtained at the higher frequencies. A detailed discussion of the results obtained at lower frequencies can be found in an earlier report.[17]

Before presenting the data that were obtained most recently, it is useful to review some of the earlier data for comparison purposes. Much of these and subsequent data were taken on a seeded plate having the types of inclusions and intended flaw locations shown in Figure 11.

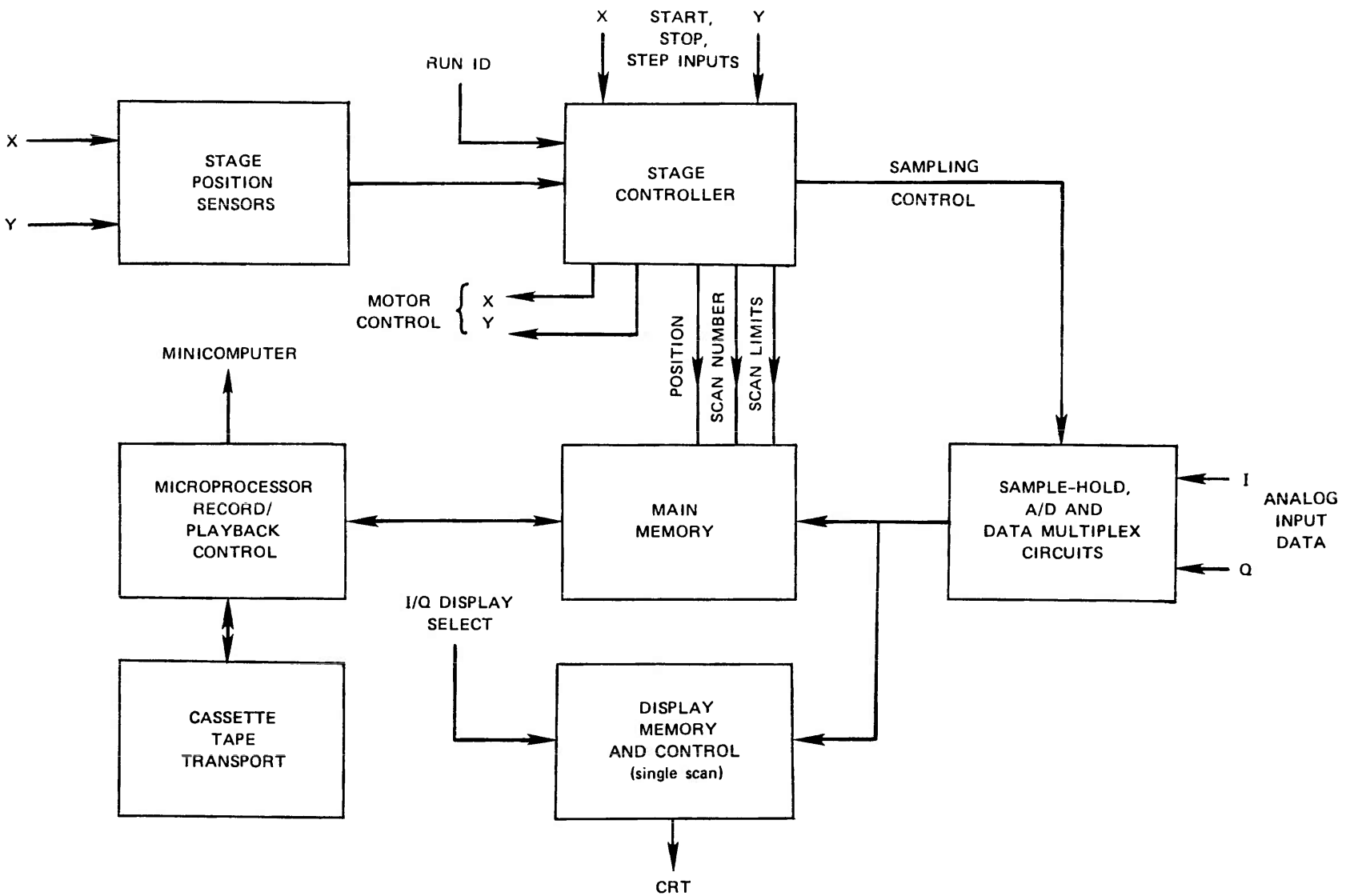

FIGURE 9 DIGITAL-STAGE-CONTROL AND DATA-ACQUISITION SYSTEM

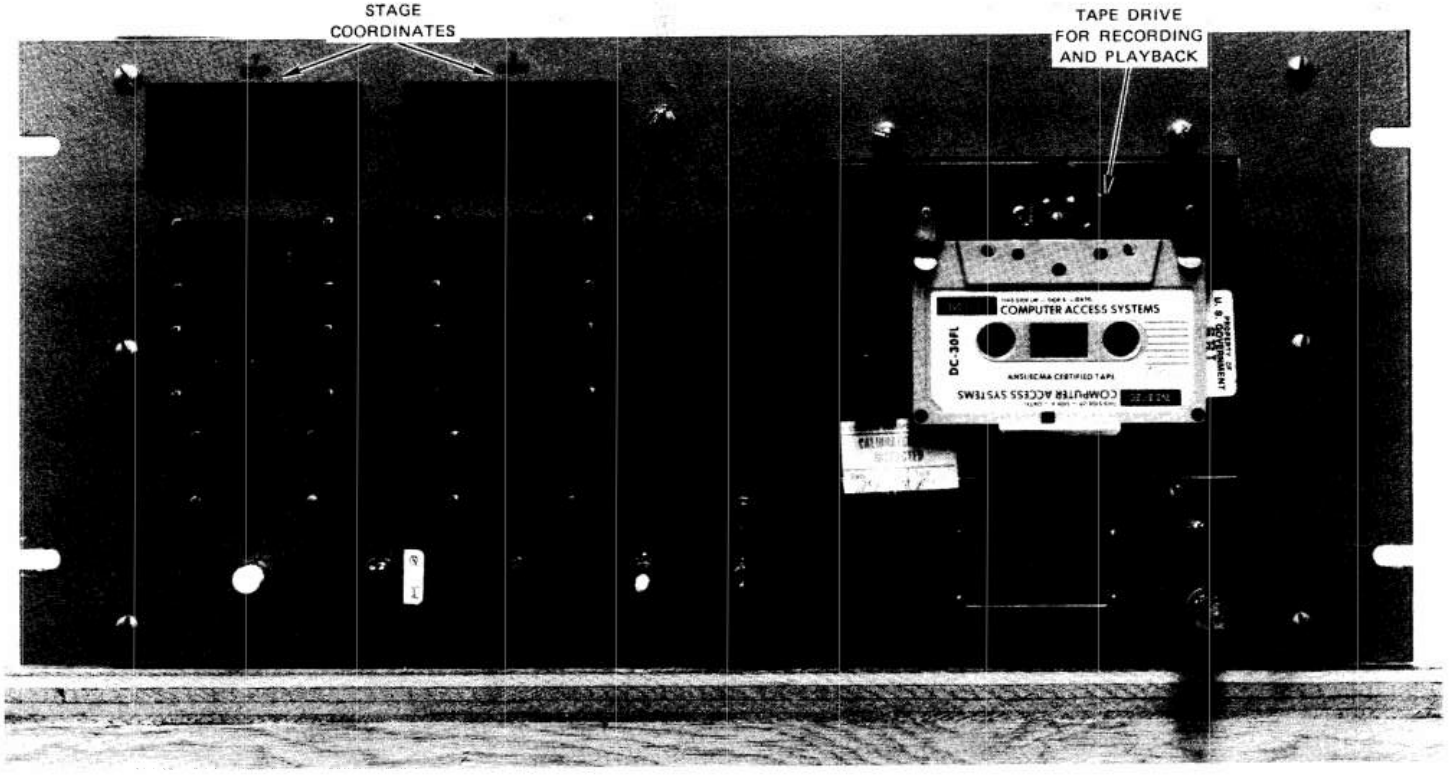

FIGURE 10 FRONT PANEL OF DIGITAL-STAGE-CONTROL AND DATA-ACQUISITION SYSTEM

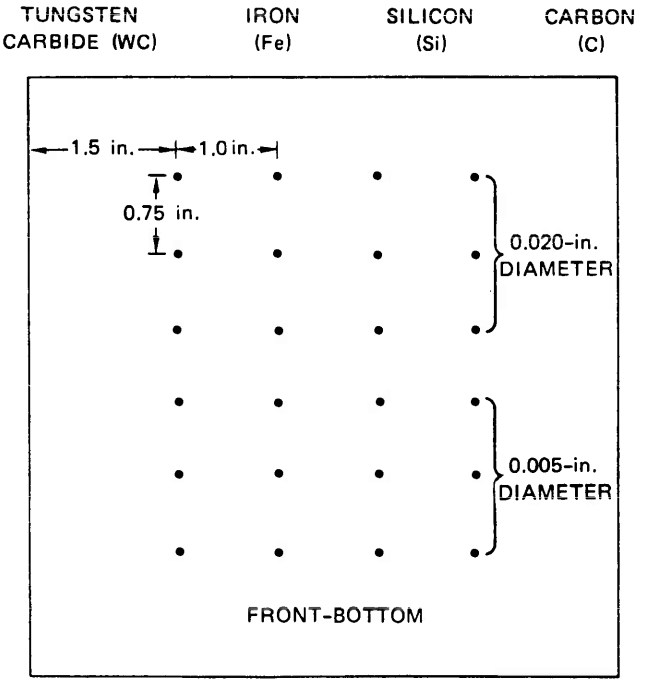

MATERIAL: HOT-PRESSED SILICON NITRIDE, NORTON NC 132
FINISH: SURFACE GROUND BOTH SIDES
SIZE: 6.25 x 6.25 x 0.25 in.

FIGURE 11 INTENDED FLAW LOCATIONS FOR SEEDED Si_3N_4 PLATE NO. 3, BILLET E307103897

The actual positions of some of the flaws were determined by the sponsor using ultrasonic C-scan* imaging, and the results are shown in Figure 12. By comparing this figure with Figure 11, one notes that some of the flaws have wandered from their intended positions, and that some unintentional flaws of undetermined type are present. About half of the intended 0.005-inch-diameter defects were not visible in the copy of the ultrasonic C-scan that was provided with the plate.

Figure 13 shows a microwave cross-polarized transmission C-scan of a 1.25 by 4.00-inch portion of this plate that contains both the 0.020-inch- and 0.005-inch-diameter inclusions. Figure 13(a) shows the area covered by the scan and the intended flaw locations. Figure 13(b) shows the portions of the scan area that produce a scattered signal greater than an arbitrarily selected threshold value (hence the term, "excess signal"). Finally, Figure 13(c) shows the amplitude of the scattered signal as a function of position within the scan area.

It can be seen that all of the 0.020-inch-diameter flaws were detected. Iron provides the strongest signal, and is the only 0.005-inch-diameter flaw that is clearly detected in this figure (some of the other small flaws can be detected if the frequency is changed). Besides being strong, the scattering from the 0.020-inch-diameter iron is spread over a relatively broad area with a diameter of about 0.5 inch. X-rays show that the iron particle has a highly irregular shape, probably produced by the hot-pressing operation. This irregular shape spreads the scattering over a wide range of angles.

A scattered signal that gives the impression of having been produced by a long, thin flaw is also apparent in Figure 13(c). This signal does not correlate with any flaw detected in this plate using either X-ray, ultrasonic, or dye-penetrant NDE techniques. More will be said later regarding this unexplained signal.

After iron, it appears that silicon produces the next largest signal. In fact, closely spaced silicon particles 0.001 inch in diameter

---

*In common usage the term "C-scan" refers to the imaging of material variations in the scanning plane.

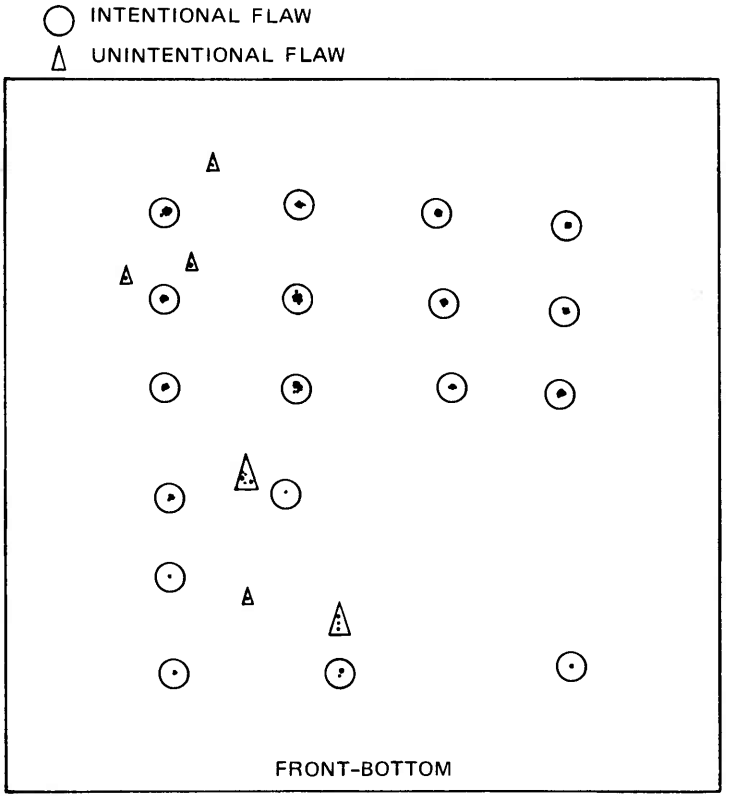

FIGURE 12 ULTRASONIC C-SCAN MAP SHOWING ACTUAL POSITIONS OF FLAWS IN Si_3N_4 PLATE NO. 3, BILLET E307103897 (25 MHz; focused transducer — some flaws were not detected)

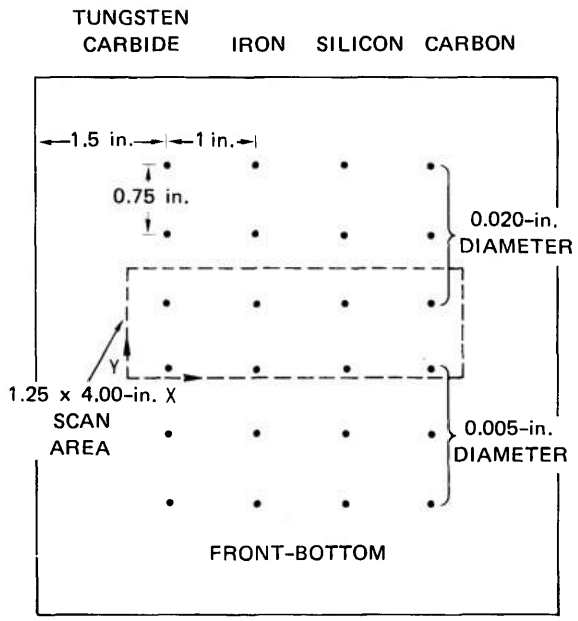

MATERIAL: Hot Pressed Silicon Nitride, Norton NC 132
FINISH: Surface Ground Both Sides

(a) MAP OF INTENDED FLAW LOCATIONS SHOWING SCAN AREA

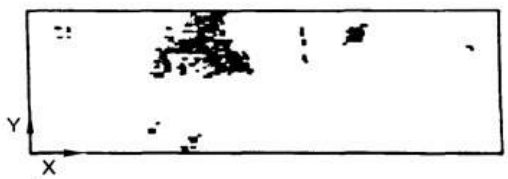

(b) EXCESS SIGNAL AS A FUNCTION OF POSITION

(c) AMPLITUDE AS A FUNCTION OF POSITION

FIGURE 13 MICROWAVE CROSS-POLARIZED-TRANSMISSION C-SCAN OF FOUR TYPES OF INCLUSIONS IN HOT-PRESSED Si_3N_4 PLATE NO. 3, BILLET E307103897 (frequency = 94 GHz)

were detected by microwave transmission measurements[17] at 98 GHz in a hot-pressed Si_3N_4 plate borrowed from AiResearch Manufacturing Company. However, the data shown in Figure 13 indicate that single silicon particles five times as large were not detectable with the present microwave system. Since silicon inclusions are particularly detrimental to the strength of Si_3N_4,[18] further development to improve the silicon-detection sensitivity of microwave NDE would appear to be worthwhile.

A reaction-sintered seeded Si_3N_4 plate was also borrowed from AiResearch Manufacturing Company. An increase in clutter level caused by this material's larger grain size and higher porosity was definitely noted. However, the clutter level did not appear to be large enough to mask detection of 0.010-inch-diameter inclusions. Small inclusions were not examined in this plate because of mechanical limitations in the scanning system that existed at the time, but, of course, the inclusions having a size equal to, or less than, the grain or pore size in the material would not be distinguishable from the background.

The same conclusion holds with regard to the effect of surface roughness. During the program, a relative comparison was made of the scattering from a disk of hot-pressed Si_3N_4 having an as-pressed, grit-blasted surface, and the scattering from the same disk after surface grinding. Qualitatively, the difference in clutter level for the two surface conditions was about the same as that observed for hot-pressed and reaction-sintered material.

To study the possibility of detecting voids as well as inclusions, microwave transmission measurements were conducted on a hot-pressed, surface-ground, Si_3N_4 plate that contained seeded voids. The voids were formed in the interior of a 0.250-inch-thick Si_3N_4 plate by first drilling small holes in a 0.125-inch-thick plate, and then diffusion-bonding this plate to a second 0.125-inch-thick plate. The measured data are shown in Figure 14. Not all the voids were detected by the microwave system, but these particular voids were also weakly imaged in an X-ray, indicating that they probably contained some kind of material rather than being empty as was intended.

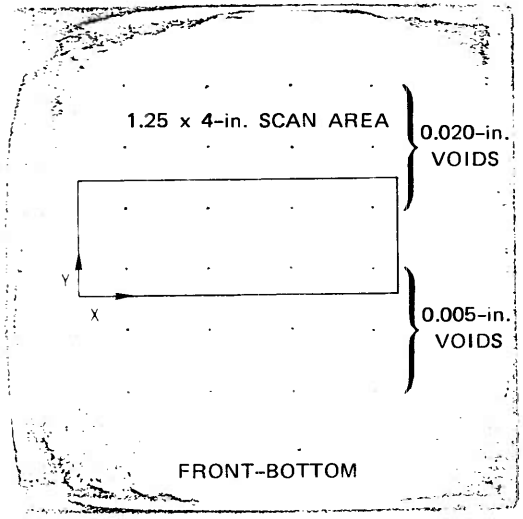

(a) ULTRASONIC C-SCAN (focused 25 MHz) MAP SHOWING VOID LOCATIONS AND SCAN AREA

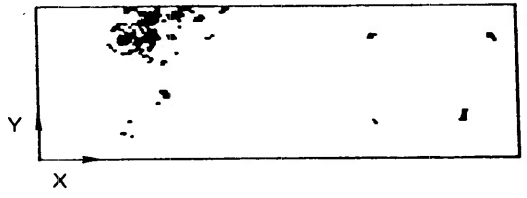

(b) EXCESS SIGNAL AS A FUNCTION OF POSITION

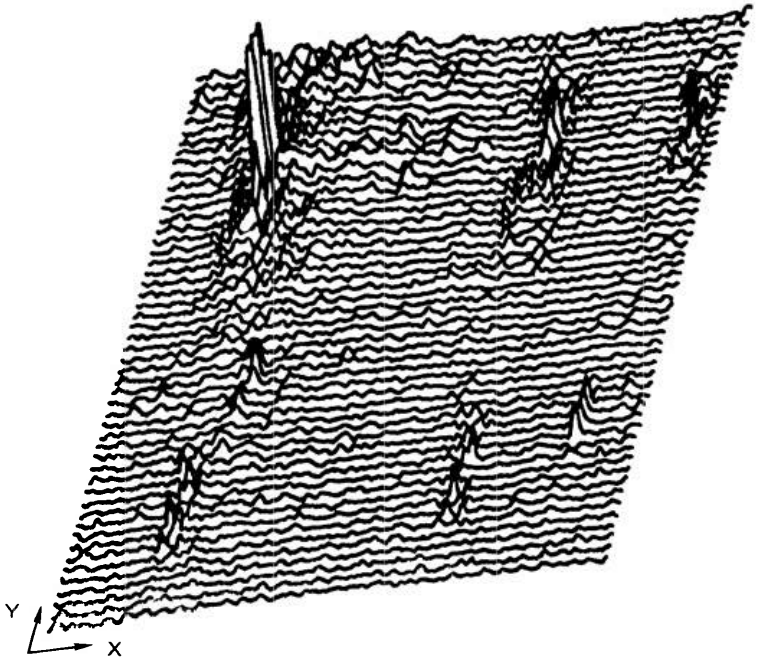

(c) AMPLITUDE AS A FUNCTION OF POSITION

FIGURE 14 MICROWAVE CROSS-POLARIZED-TRANSMISSION C-SCAN OF VOIDS IN HOT-PRESSED Si_3N_4 PLATE, BILLET F307104930 (frequency = 94 GHz)

As was remarked earlier, all of these data were taken using open-ended-waveguide antennas and a rudimentary X-Y stage with limited area coverage. Some of the microwave cross-polarized transmission C-scans were repeated in the latter half of the program after the system shown in Figures 7, 8, and 10 was completed. The transmission data obtained using this new system were acquired under conditions that differed in three major respects from the conditions that prevailed during the earlier experiments:

(1) The new transmitting antenna was a lens-focused horn located 3 inches from the plate surface.

(2) The radiated power was lower by about 10 dB.

(3) The areas inspected were larger.

Cross-polarized transmission data taken at 100 GHz for plate No. 3, billet E307103897, are shown in Figure 15. Figure 15(a) shows the detected amplitude as a function of position for six contiguous scan areas that together form a 5-inch-square area encompassing all the seeded inclusions (see Figure 11). These scan areas are labeled 1 through 6, beginning at the bottom of the plate where the smaller inclusions are located. The physical separation between scan lines is 0.020 inch. The smallest detectable signal in these data was about -40 dBm (determined by electronic system noise). Scans 3 and 4 in Figure 15(a) cover about the same area as that which is shown in Figure 13. The data shown in these two figures are very similar, except that the signal-to-noise ratio is somewhat poorer in the new data because of the smaller available power and the increased gain.

Although the plots shown in Figure 15(a) give a good idea of how the signal amplitude varies with position, they are not very convenient for determining the number and actual locations of the detected signals. A better plot for this purpose is shown in Figure 15(b), where the dark points indicate the positions on the plate where the signal exceeds a threshold value (usually chosen just slightly larger than the noise or clutter signal), but smaller than an upper limit that is typically chosen to be 2 to 10 times the threshold value. Thus, this plot depicts a "slice" through the amplitude as a function of position, and is called

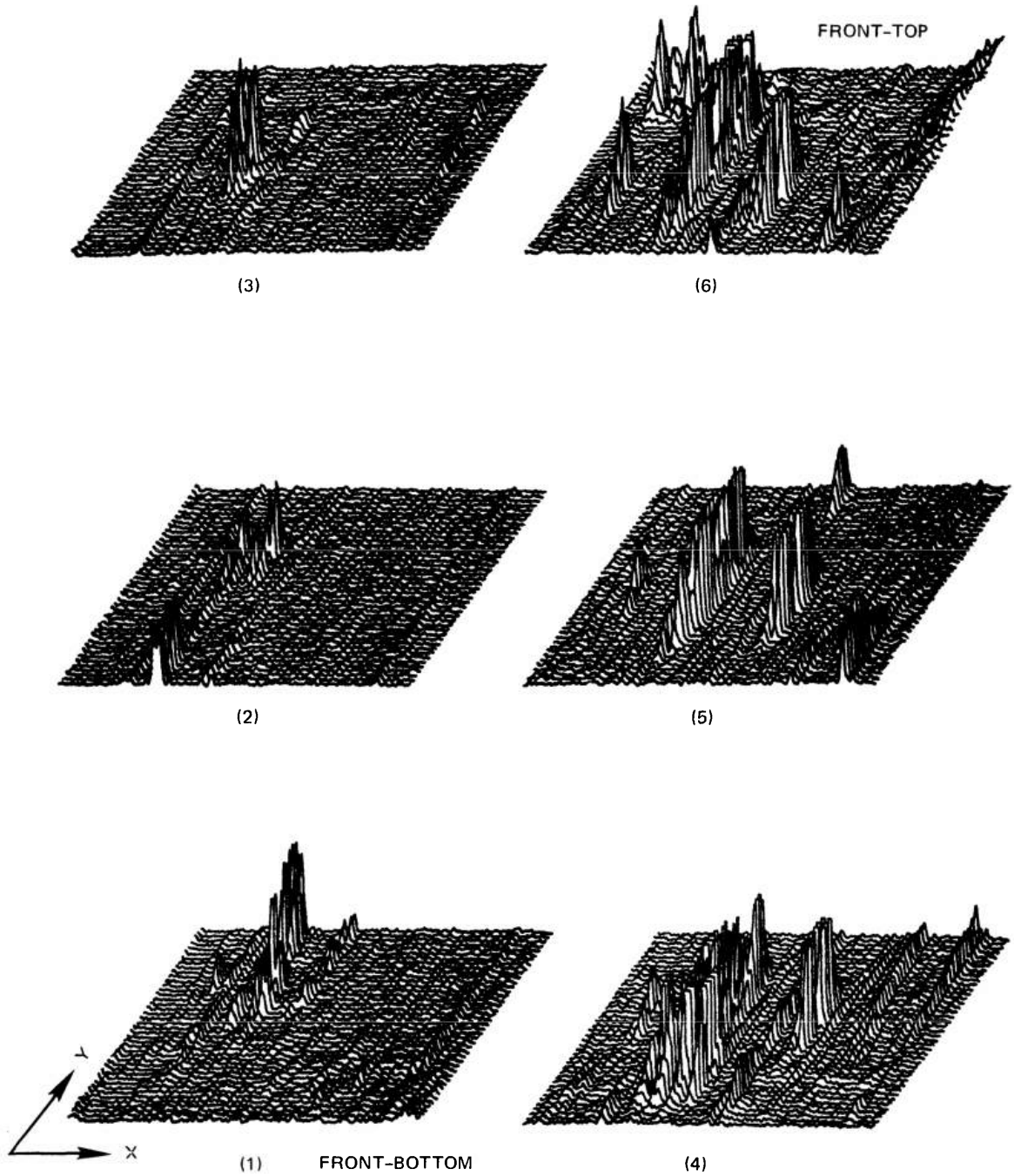

(a) AMPLITUDE AS A FUNCTION OF POSITION (each scan area is 5.0 x 0.8 in.)

FIGURE 15 MICROWAVE CROSS-POLARIZED-TRANSMISSION C-SCAN OF SEEDED HOT-PRESSED Si_3N_4 PLATE NO. 3, BILLET E307103897 (frequency = 100 GHz)

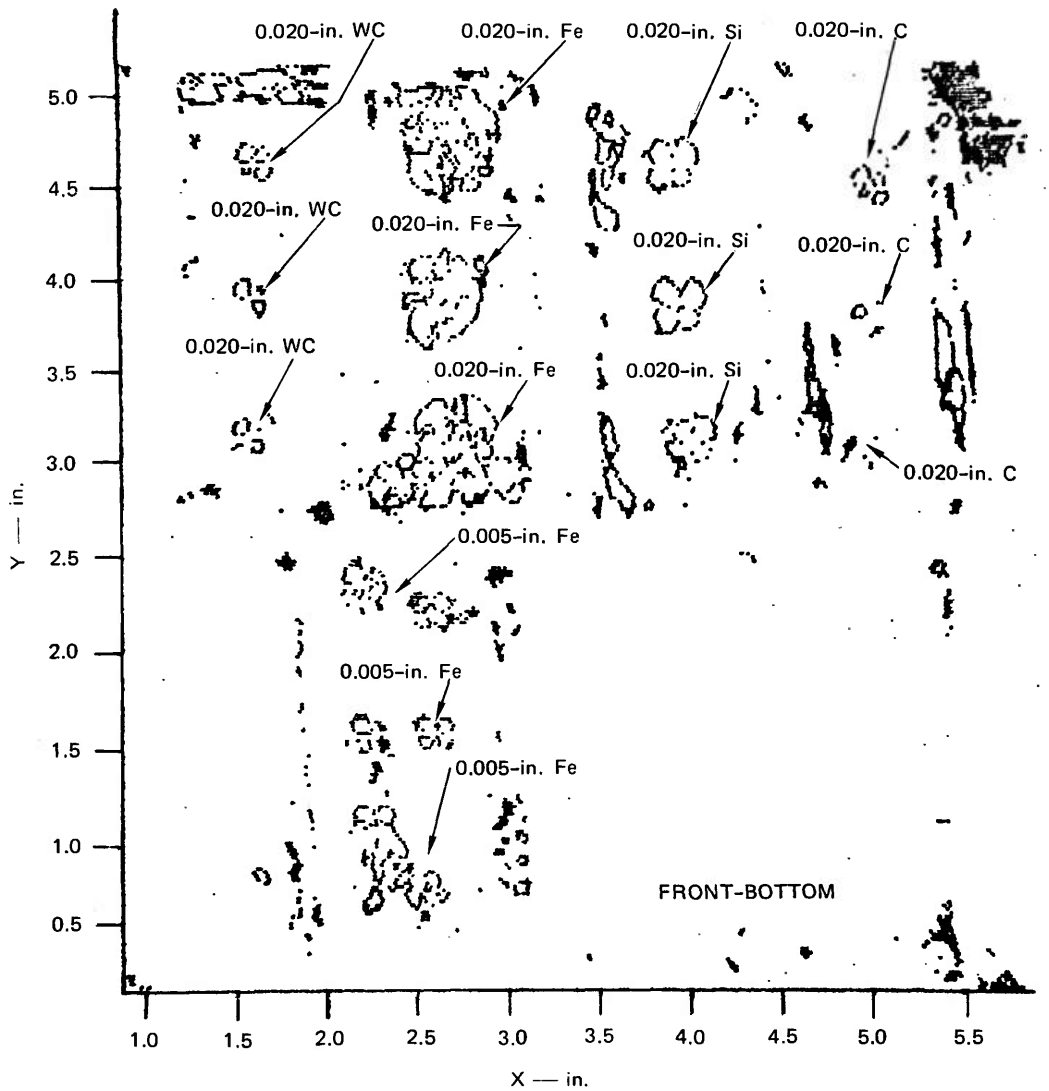

(b) EXCESS-SIGNAL CONTOUR (5.0 x 5.0-in.-scan area, plate center 3.4 in., 2.7 in.)

FIGURE 15 MICROWAVE CROSS-POLARIZED-TRANSMISSION C-SCAN OF SEEDED HOT-PRESSED Si_3N_4 PLATE NO. 3, BILLET E307103897 (frequency = 100 GHz) (Concluded)

an excess-signal contour. The X and Y coordinates in Figure 15(b) are stage coordinates that are defined by the stage-controller system. Conversion to plate coordinates is accomplished by locating a point on the plate in stage coordinates. For example, the center of the plate can be located by removing the plate and placing a waveguide probe at the position of the plate center. Then the stage coordinates are noted when the stage is in a position that maximizes the energy received by the probe.

Figure 15(b) shows that all of the 0.020-inch inclusions were detected, with iron producing the strongest signal, and carbon the weakest. The signal produced by the iron extends over an area with a diameter of about 0.5 inch, while the spatial extent of the signal produced by the silicon is about 0.25 inch. The observed spatial extent of the signal is determined by (1) the sizes of the transmitting and receiving beams at the inclusion, (2) the scattering characteristics of the flaw, and (3) the detection threshold.

Inspection of the area containing the smaller 0.005-inch inclusions shows that the only signals detected are in the region that supposedly contains iron. There appear to be two particles in each row, rather than the single particles that were to be put in by the manufacturer of the plate.

In addition to the signals that correlate with the known presence of inclusions, several other signals were detected that do not correlate with any of the known flaws. A large signal appears in the upper-left-hand corner of the plate, just above the uppermost tungsten carbide inclusion. Also, there are several narrow ridge-like signals that are aligned parallel to the Y axis. More will be said later about these latter signals.

Before discussing other data, one other potentially important feature of these data should be mentioned--the "four-leaf-clover" pattern produced by the silicon inclusions and also by some of the tungsten carbide and carbon particles. The orientation of this pattern in the C-scan is determined by the direction of the polarization of the illuminating wave. Hence, the observed pattern is a bona fide scattering pattern characteristic of these inclusions.

A plausible explanation for the observed scattering behavior follows from the Mie theory for the scattering of plane electromagnetic waves by conducting or dielectric spheres.[19] In that theory, the scattering is written as a sum of partial waves, or modes. The electric field patterns for the first two of these modes are shown in Figure 16. The amplitudes with which these modes are excited diminish rapidly when the order of the mode exceeds $2\pi a/\lambda$, where a is the radius of the sphere and λ is the wavelength. Since $2\pi a/\lambda < 1$ for all the cases of interest here, a linearly polarized incident wave excites the first-order (dipole) mode [Figure 16(a)] most strongly. However, this mode does not couple to a cross-polarized receiving antenna. Hence, for spherical scatterers one must rely on detecting the weakly excited second-order (quadripole) mode [Figure 16(b)] when using a cross-polarized system. Consideration of the inherent symmetries in this mode shows that the cross-polarized scattering pattern produced by this mode should be exactly like the observed pattern. Even though most of the actual inclusions of interest are not exactly spherical, they are small enough compared with a wavelength so that they can be approximated as spherical. Hence, it appears

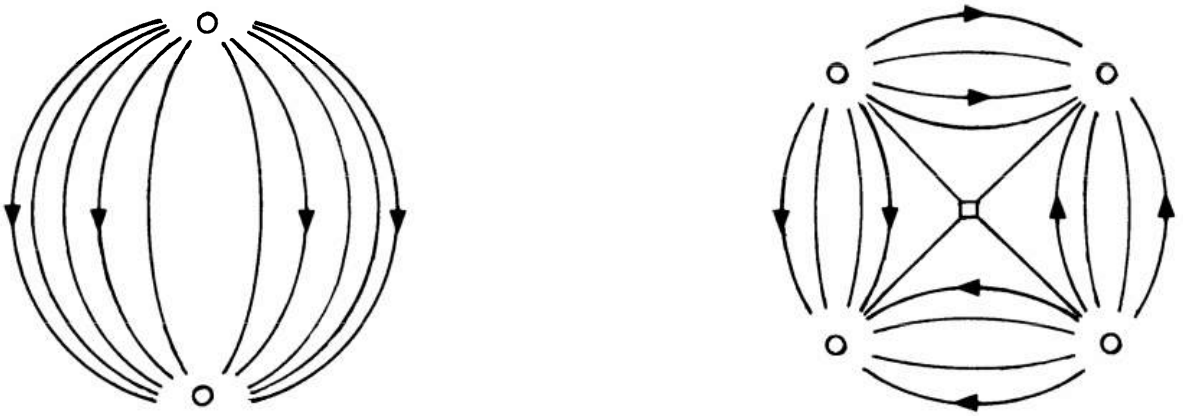

(a) DIPOLE MODE (b) QUADRIPOLE MODE

FIGURE 16 ELECTRIC FIELD PATTERNS FOR THE FIRST TWO MODES USED IN DESCRIBING THE SCATTERING FROM A SPHERE

that excitation and detection of the quadripolar mode is the basic physical mechanism involved in the detection of small inclusions in ceramic material using a cross-polarized transmission system.

The clover-leaf scattering patterns in Figure 15(b) that are produced by the silicon inclusions (a silicon inclusion is typically round and flat like a pancake) are easily distinguished from the patterns produced by the jagged iron inclusions. This feature may prove useful for determining the type of flaw that has been detected.

A second hot-pressed Si_3N_4 plate seeded with spherical 0.025-inch-diameter tungsten carbide particles was also examined using the new cross-polarized microwave transmission system. The relative flaw locations in this plate (as determined by an X-ray) are shown in Figure 17. The spacing between flaws was varied in this plate so that the plate could be used to test the spatial resolution of the 100-GHz system.

The measured amplitude as a function of position is shown for this plate in Figure 18(a). The data are shown in six contiguous scans that cover the area containing the inclusions. The tungsten carbide particles are weak scatterers, and are barely detectable with the transmission system. As in the other plate, several unexplained signals also exist.

The ability of the microwave system to resolve these flaws is best determined from the excess-signal contour shown in Figure 18(b). All of the inclusions are resolved in this figure, including those having the closest spacing, namely 0.3 inch. Some confusion in determing the flaw location without a prior knowledge would occur, however, because of the very weak signals and correspondingly poor signal-to-noise ratio obtained in this case.

Both plates examined with the new microwave system produce a number of signals that do not correlate with known flaws. The magnitudes of these unexplained signals depend on the orientation of the incident polarization with respect to the plate axes. The data shown in Figures 15 and 18 were taken with the electric polarization aligned along the Y axis. Data that compare the results obtained from this polarization to that obtained with the polarization oriented at 45° to the Y-axis

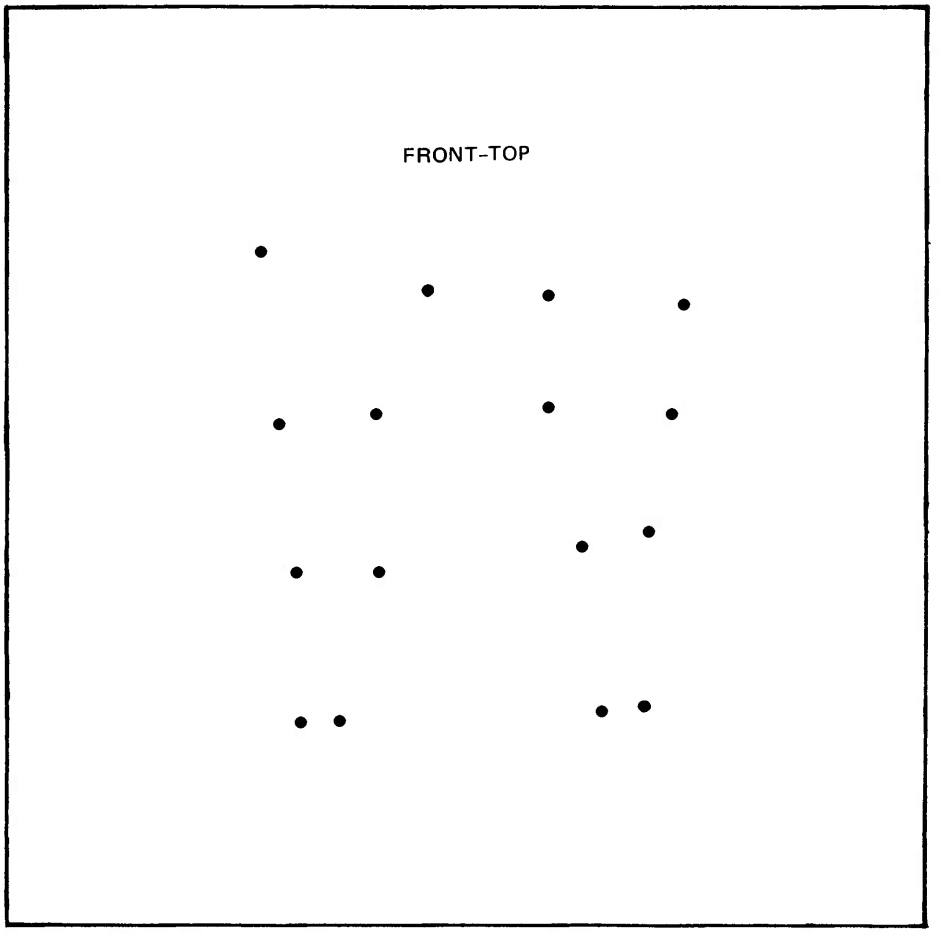

MATERIAL: HOT-PRESSED SILICON NITRIDE, NORTON NC 132
FINISH: SURFACE GROUND BOTH SIDES
SIZE: 6.25 x 6.25 x 0.25 in.

FIGURE 17 FLAW PATTERN IN SEEDED Si_3N_4 PLATE NO. D200974 — 1158
(all flaws are 0.025-in. diameter tungsten carbide)

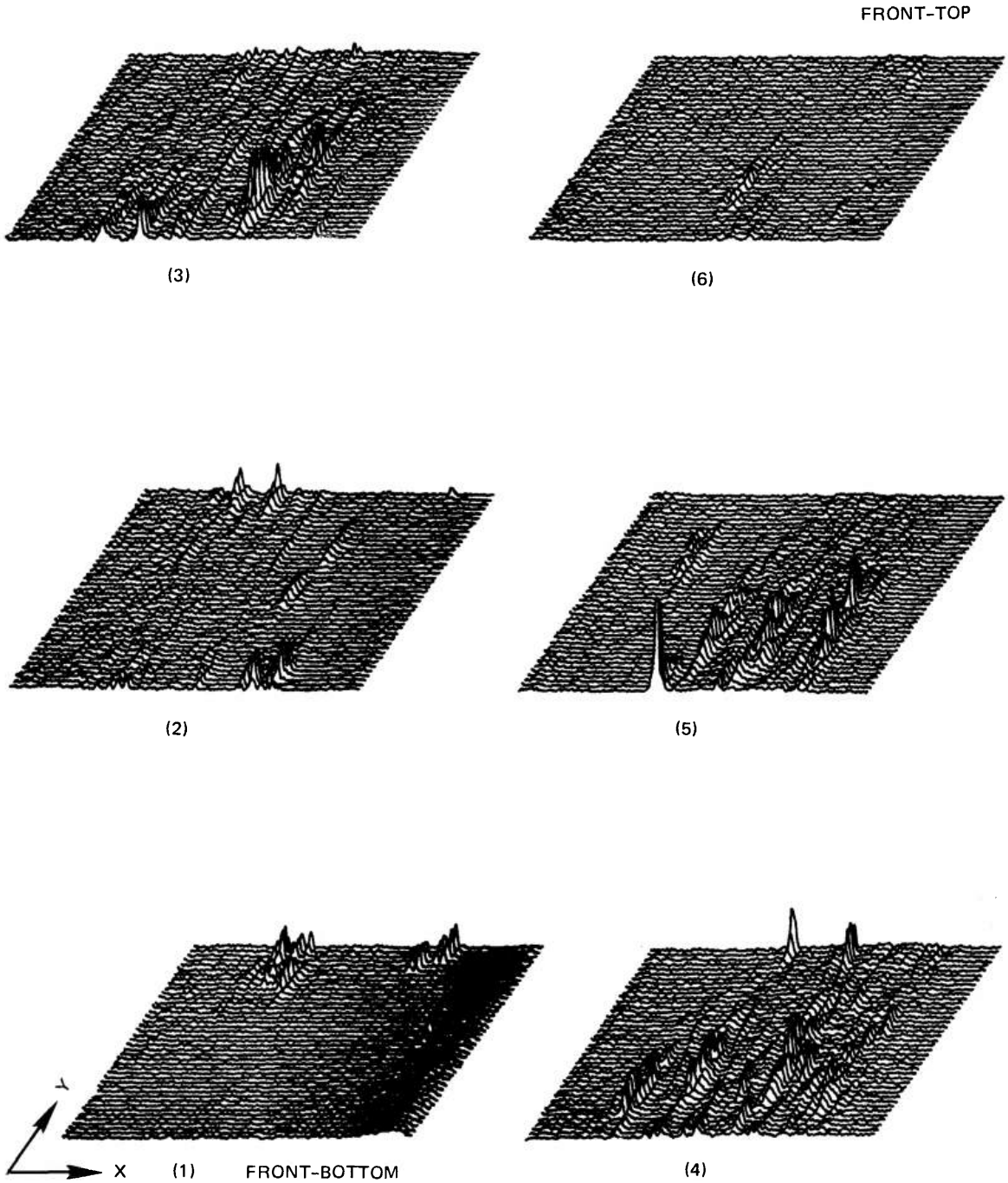

(a) AMPLITUDE AS A FUNCTION OF POSITION (each scan area is 5.0 x 0.8 in.)

FIGURE 18 MICROWAVE CROSS-POLARIZED-TRANSMISSION C-SCAN OF SEEDED HOT-PRESSED Si_3N_4 PLATE NO. D200974-1158 (frequency = 100 GHz)

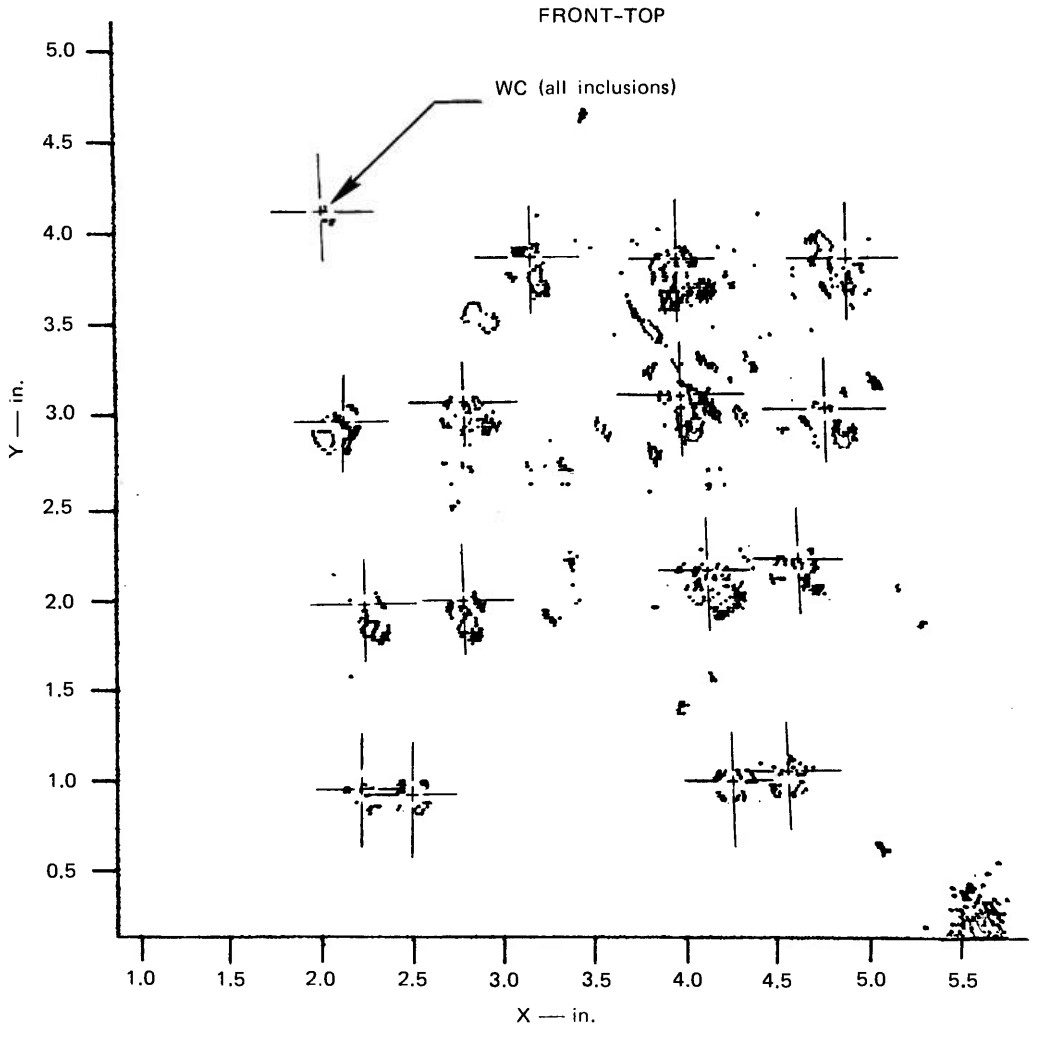

(b) EXCESS-SIGNAL CONTOUR (5.0 x 5.0-in. scan area, plate center = 3.4 in., 2.7 in.)

FIGURE 18 MICROWAVE CROSS-POLARIZED-TRANSMISSION C-SCAN OF SEEDED HOT-PRESSED Si_3N_4 PLATE NO. D200974-1158 (frequency = 100 GHz) (Concluded)

are shown in Figures 19 and 20. For both plates, the unexplained signals are much larger when the polarization is oriented at 45° to the plate axes. Also, the spatial characteristics of these signals differ for the two plates. In Figure 19(a) the "extra" signals appear mostly as thin "ridges" aligned with the Y-axis,* whereas in Figure 20(a) they appear mostly as localized "spikes." The positions of these extra signals relative to the plate do not change when the plates are turned over or rotated by 90°. Hence, one can conclude these signals are not caused by spurious scattering from the X-Y stage structure. One may also conclude that whatever produces them is associated with the plate, and has a linear symmetry axis aligned along the Y-axis (i.e., the scattering source is not spherically symmetric).

One possible cause for these unexplained signals could be density striations in the hot-pressed plates. However, proof of whether these signals are flaw-related or measurement-related cannot be obtained until destructive tests are performed. Such tests were not within the scope of the present program.

All of the data discussed so far were obtained with a cross-polarized transmission system, using either two open-ended-waveguide antennas or one focused-horn antenna as a transmitter and one open-ended waveguide as a receiver. This system requires that the two antennas be aligned axially and that the open-ended waveguide antenna be as close to the surface of the sample as possible to minimize beam spreading. These requirements lead to a need for tight mechanical tolerances and lengthen the set-up time. Therefore, it was reasoned that a far-field backscatter measurement using only one antenna (the lens-focused horn) should not suffer these problems. It is also convenient to use coherent (homodyne) detection in such a system, thereby providing both amplitude and phase information. A block diagram of such a backscatter system is shown in Figure 5(b) and a photograph of the same system in Figure 7.

---

*Note, however, that there are two very large unexplained "spikes" in the upper-right-hand corner of Figure 19(a).

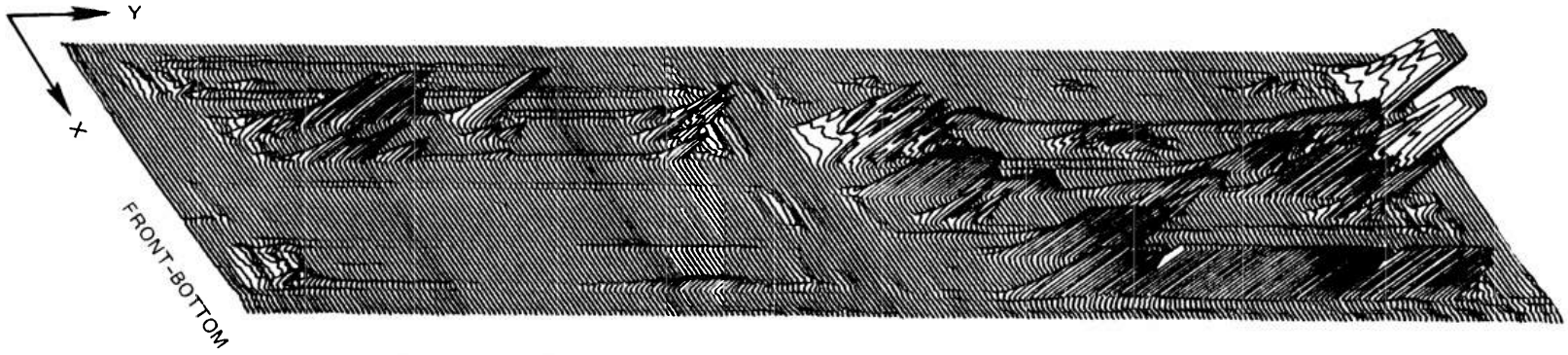

(a) FREQUENCY = 100.5 GHz, SENSITIVITY ≃ -30 dBm, POLARIZATION AT 45° TO Y-AXIS

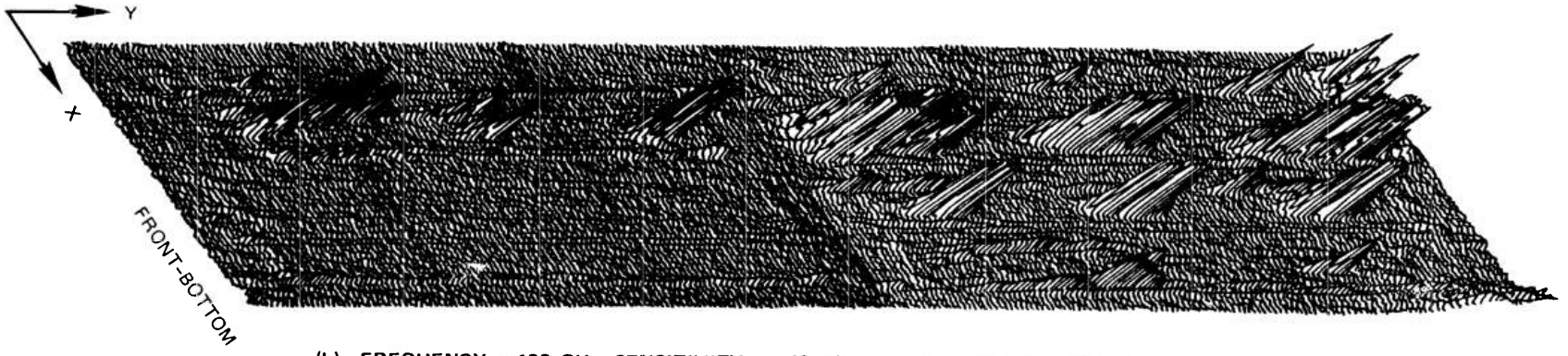

(b) FREQUENCY = 100 GHz, SENSITIVITY ≃ -40 dBm, POLARIZATION ALONG Y-AXIS

FIGURE 19 MICROWAVE CROSS-POLARIZED-TRANSMISSION C-SCANS OF SEEDED HOT-PRESSED Si_3N_4 PLATE NO. 3, BILLET E307103897 · AMPLITUDE AS A FUNCTION OF POSITION (5.0 x 5.0-in. scan area)

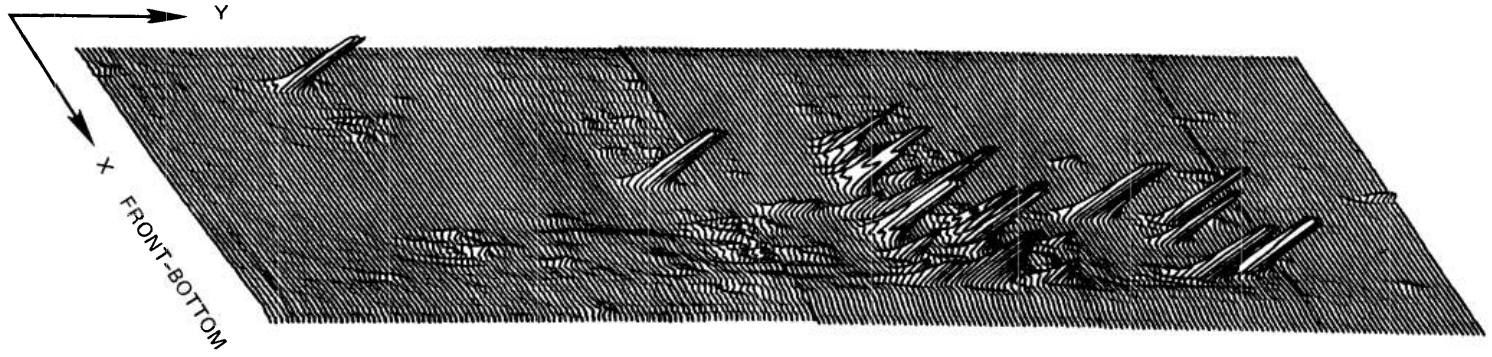

(a) FREQUENCY = 100.5 GHz, SENSITIVITY ≃ -30 dBm, POLARIZATION AT 45° TO Y-AXIS

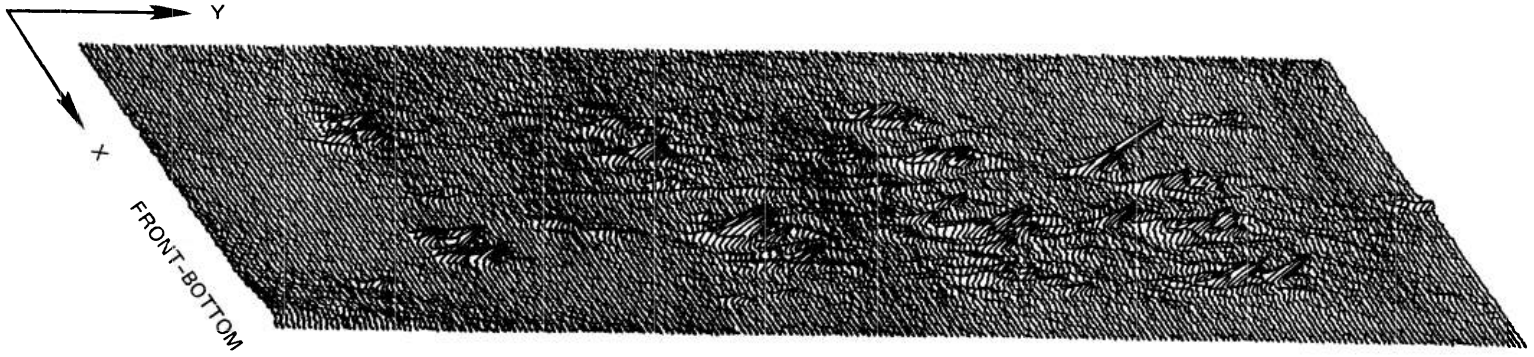

(b) FREQUENCY = 100 GHz, SENSITIVITY ≃ -40 dBm, POLARIZATION ALONG Y-AXIS

FIGURE 20 MICROWAVE CROSS-POLARIZED-TRANSMISSION C-SCANS OF SEEDED HOT-PRESSED Si_3N_4 PLATE NO. D200974-1158 — AMPLITUDE AS A FUNCTION OF POSITION (5.0 x 4.5-in. scan area)

Unfortunately, two new problems were encountered with the backscatter system that rendered it less useful than the transmission system: (1) the cross-polarized backscatter from the flaws was found to be smaller than the forward scatter, and (2) the clutter rejection obtainable using the orthomode coupler was less than that which could be achieved using the two cross-polarized antennas. Thus, measurements performed with this system exhibited a poorer signal-to-clutter ratio that made detection of the inclusions in the seeded plates difficult. Also, only the amplitude data were of any use; the phase data were too erratic for them to be interpreted meaningfully.

Backscatter amplitudes as functions of position are shown in Figures 21 and 22 for the two seeded plates examined previously by the transmission method. Figure 21 should be compared with Figure 19(a), and Figure 22 with the left half of Figure 20(b). In Figure 21, the signals caused by the iron inclusions are just discernible above the clutter. It is interesting to note that some of the unexplained signals discussed previously are also present in the backscatter. In Figure 22, the data were taken with 10 dB more sensitivity than those shown in Figure 20(b), but the backscatter caused by the tungsten carbide inclusions is barely visible above the clutter. The clutter in Figure 22 also varies significantly during an X-axis scan--an effect that could be caused by a slight tilt of the plate or by variations in the density or thickness of the plate. Hence, it appears that transmission (or, in general, bistatic) measurements are to be preferred for the microwave NDE of ceramics unless the sensitivity (clutter rejection) of backscatter measurements can be improved.

One final point with regard to using cross-polarized microwave scattering to detect flaws in ceramics concerns the amount of scattering produced by the edges of the sample. The experiments have shown that such geometric discontinuities do indeed produce a large amount of scattering, and therefore the technique cannot be used to inspect for flaws near such edges. The closest point to an edge that can be approached without degrading sensitivity is determined by the antenna beam patterns.

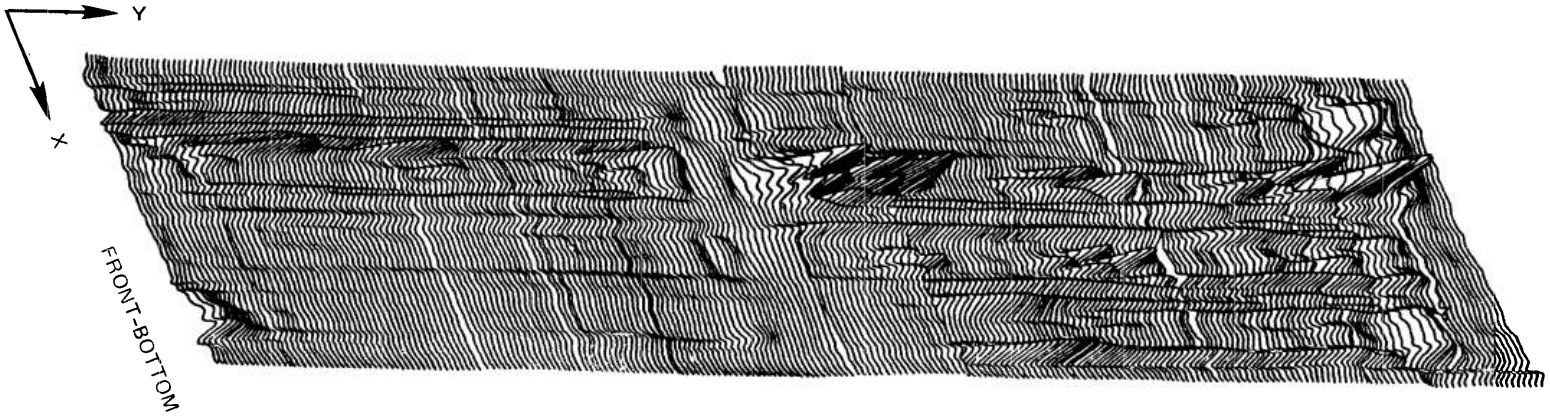

AMPLITUDE AS A FUNCTION OF POSITION (frequency = 101 GHz, sensitivity ≃ -40 dBm, polarization at 45° to Y-axis)

FIGURE 21 MICROWAVE CROSS-POLARIZED-REFLECTION C-SCAN OF SEEDED HOT-PRESSED Si_3N_4 PLATE NO. 3, BILLET E307103897 (5.0 x 4.9-in. scan area)

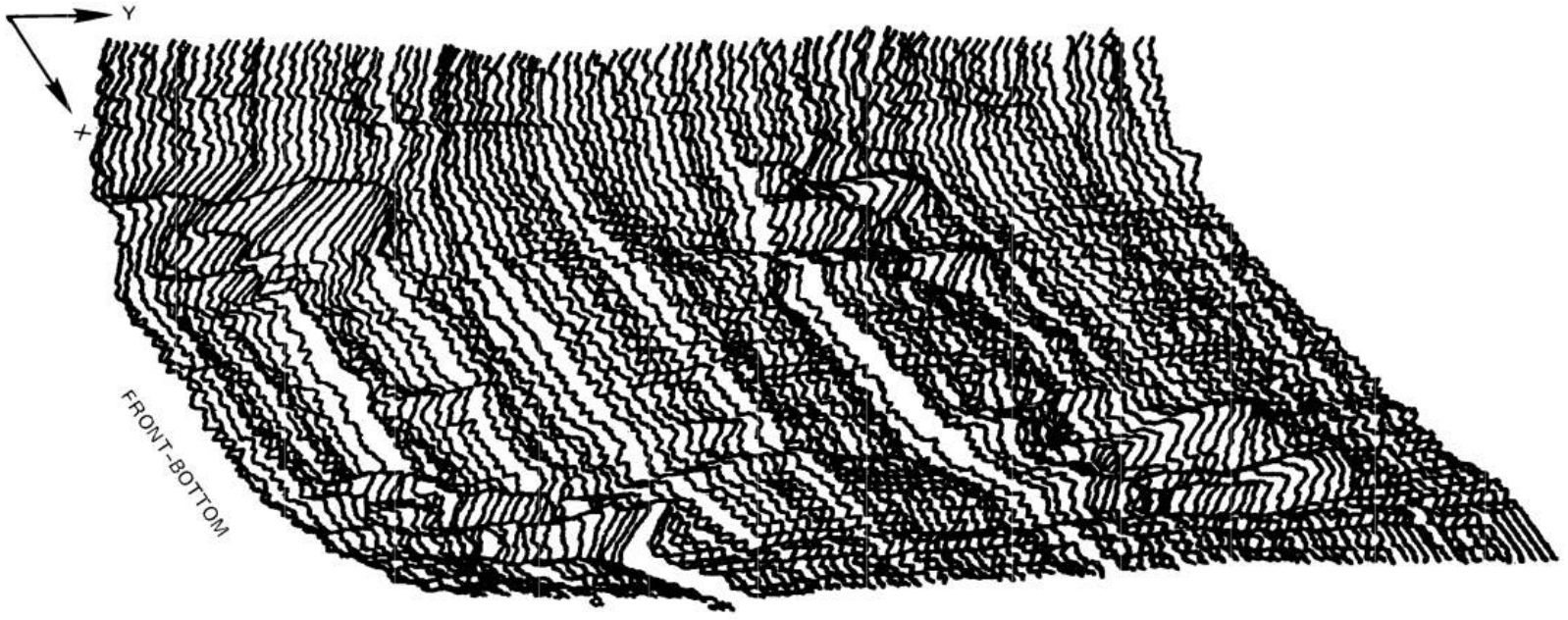

AMPLITUDE AS A FUNCTION OF POSITION (frequency = 101.6 GHz, sensitivity ≃ -50 dBm, polarization along Y-axis)

FIGURE 22 MICROWAVE CROSS-POLARIZED-REFLECTION C-SCAN OF SEEDED HOT-PRESSED Si_3N_4 PLATE NO. D200974-1158 (4.0 x 2.0-in. scan area in lower part of plate)

Data that illustrate the effect of an edge are shown in Figures 23 and 24. The samples used for these tests were two hot-pressed Si_3N_4 disks, 1 inch in diameter, that were borrowed from the Rockwell International Science Center.* The thickness of both disks was 0.240 inch, and the broad surfaces of the disks were ground smooth and flat. However, the edges of the disks were left in the rough, as-pressed condition. Sample number 124 (Figure 23) contained a centrally located 0.005-inch-diameter silicon inclusion and sample number 132 a 0.008-inch-diameter silicon inclusion.

The edge scattering is very large in both cases. The effect of the edge scattering is noticeable about 0.3 inch from the edge--about 2 beam widths for the focused horn. Weak signals are detectable near the centers of the disks, possibly caused by the silicon inclusions. However, because the strong edge scattering produces small ripples at a considerable distance from the rough edges, one cannot draw a definite conclusion from these data concerning the presence of the silicon inclusions.

*Courtesy of Dr. A. G. Evans.

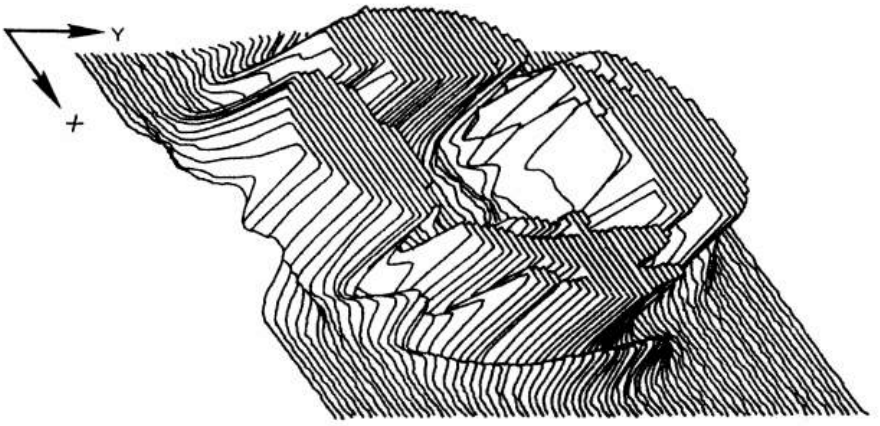

(a) AMPLITUDE AS A FUNCTION OF POSITION (1.5 x 1.5-in. scan area)

(b) AMPLITUDE AS A FUNCTION OF POSITION (view of central portion of disk)

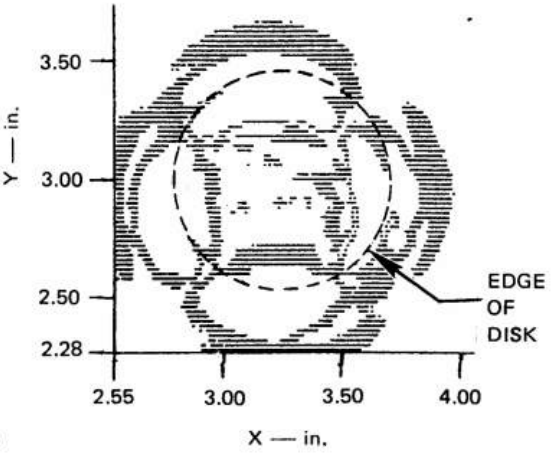

(c) EXCESS-SIGNAL CONTOUR (1.5 x 1.5-in. scan area)

FIGURE 23 MICROWAVE CROSS-POLARIZED-TRANSMISSION C-SCAN OF 1-in.-DIAMETER HOT-PRESSED Si_3N_4 DISK, ROCKWELL SAMPLE NO. 124, (frequency = 100 GHz, sensitivity $\simeq$ -40 dBm)

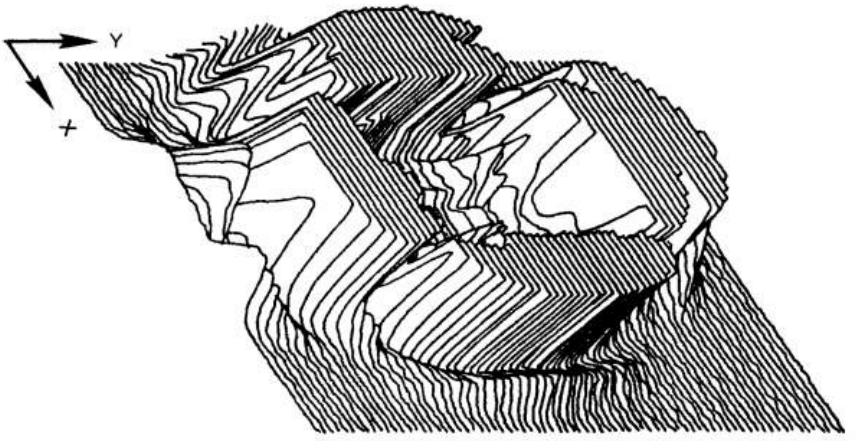

(a) AMPLITUDE AS A FUNCTION OF POSITION (1.5 x 1.5-in. scan area)

(b) AMPLITUDE AS A FUNCTION OF POSITION (view of central portion of disk)

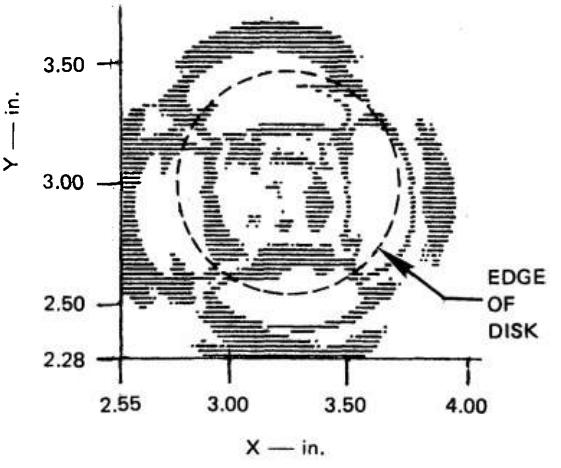

(c) EXCESS-SIGNAL CONTOUR (1.5 x 1.5-in. scan area)

FIGURE 24 MICROWAVE CROSS-POLARIZED-TRANSMISSION C-SCAN OF 1-in.-DIAMETER HOT-PRESSED Si_3N_4 DISK, ROCKWELL SAMPLE NO. 132, (frequency = 100 GHz, sensitivity $\simeq$ -40 dBm)

V THE PRACTICAL UTILITY OF MICROWAVE NDE FOR CERAMICS

A. General

The basic objective of this study and evaluation program has been to determine whether microwave scattering measurements can be usefully applied to the nondestructive evalution of ceramic components. In the previous sections of this report the basic considerations involved in answering this question have been discussed, and relevant experimental data obtained in an idealized laboratory situation have been presented. In this section the additional considerations involved in the transfer of a laboratory NDE technique to the real-world environment are discussed.

B. Limitations Imposed by Material Characteristics

The material characteristic having the greatest impact on microwave NDE is the propagation loss. The two physical mechanisms that contribute to this type of loss are electronic dissipation and grain-boundary (or surface-irregularity) scattering.* Dissipation loss appears to be negligible in Si_3N_4 at 100 GHz. However, early experiments with the one sample of SiC that was available indicate that this material is highly attenuating. Similarly, grain-boundary scattering appears to be low at 100 GHz in hot-pressed Si_3N_4; it is noticeable, but tolerable, in reaction-sintered material.

The data shown in Table 1 suggest that 0.5 dB/mm is a conservative estimate for the attenuation in hot-pressed Si_3N_4 at 100 GHz. Hence, it should be possible to inspect for internal flaws in samples that are at least 25 mm thick. Of course, the actual thickness limit caused by

---

*Grain-boundary and surface-irregularity scattering also result in increased clutter, which reduces the flaw-detection sensitivity.

attenuation will depend on the amount of power available from the transmitter and on the receiver sensitivity.

A large amount of propagation loss in the material, however, will not prevent microwave NDE from being used to inspect for flaws located on the surface of a ceramic component.

C. Sample Geometry

The data presented in this report were all obtained using samples fabricated in the form of flat plates. This type of sample permits one to take advantage of selective mode conversion to reject the clutter caused by scattering from the sample surfaces. To accomplish this clutter rejection requires that the plate be aligned with its broad surfaces perpendicular to the direction of the illuminating wave. Otherwise, tiling the plate would cause the polarization of the incident wave to be rotated (see Figure 1), and hence some of the linearly polarized incident wave would be coupled into the orthogonal mode.

A qualitative evaluation of the effect of sample tilt was attempted by tilting the X-Y stage. This procedure did not work very well for the transmission system, because the receiving antenna was rigidly attached to the stage support (see Figure 8), and thus the two antennas could not be kept sufficiently aligned along their beam axes. However, it was clear that a very slight tilt produced a significant increase in clutter, and rotating the receiving antenna to adjust its polarization was not effective in reducing the clutter to its original level.

It was possible to tilt the plate over larger angles when using the backscatter mode of operation. However, the clutter observed using this mode was even more sensitive to plate tilt than for the transmission mode because the clutter in this case is the phasor sum of the direct leakage through the orthomode coupler and the indirect leakage caused by the specular reflection from the plate. A slight tilt of the plate (other than about the scan axis) causes the phase of this indirect clutter signal to change significantly as the plate is scanned, thereby causing the net clutter signal to vary over a wide range.

It can be concluded from these results that, as long as the transmitted or specularly reflected signal is allowed to enter the receiving antenna, the use of mode conversion is only an effective clutter-rejection technique if the sample is a plate with plane, parallel faces. Hence, it appears that some important engineering components such as turbine blades are not amenable to the mode-conversion microwave NDE techniques studied during this program.

The choice of antenna arrangements used during this program was determined in part by mechanical convenience, and in part by the availability of components. Though more complicated to implement, a bistatic antenna arrangement like that shown schematically in Figure 3(b) might overcome the clutter problems discussed above. Two lens-focused horns with low sidelobes could be arranged in this scheme so that the specularly reflection(s) from the sample surface(s) is (are) aimed away from the receiving horn. The antennas could also be copolarized. The clutter rejection achievable in this way would depend on how drastically the surface geometry varied in the area being inspected. Of course, for a flaw to be detected it would have to scatter energy into the receiving antenna.

On the other hand, none of the clutter-rejection techniques that have been discussed can reject the scattering produced by a sharp edge on the sample. Hence, microwave NDE is most easily applied to inspecting for flaws that are located at least one to two free-space wavelengths (3 to 6 mm at 100 GHz) from such an edge. In some cases, however, it may be possible to use coherent processing techniques to mitigate the edge-scattering problem.

D. Sensitivity

The sensitivity of both of the systems that were tested was determined primarily by clutter. The transmission system was more sensitive to flaws, apparently because the cross-polarized forward scatter from the flaws was larger than the cross-polarized backscatter. Based on the experimental data, the detectability of various types and sizes of inclusions can be ranked in terms of minimum detectable flaw size as follows (for a single flaw):

(1) Iron: 0.005 inch (125 μm)

(2) Silicon: 0.010 inch (250 μm)

(3) Tungsten carbide: 0.020 inch (500 μm)

(4) Carbon: 0.020 inch (500 μm)

(5) Cylindrical void: 0.020 inch (500 μm)

Surface cracks are another important flaw that occurs in ceramic materials. Some cracks were artifically initiated in a sample of hot-pressed Si_3N_4 using a Knoop indenting tool. The largest of these was about 0.050 inch (1250 μm) in length. However, none could be detected with the cross-polarized microwave systems, presumably because the volumes of such cracks are relatively small for frequencies involved. It might be possible to enhance the microwave detection of surface cracks by applying a penetrating conducting liquid to the surface.

If the transmit-receive isolation (clutter rejection) could be improved, the flaw-detection sensitivity of the homodyne receiver could be increased by raising the tramsitter power, or, alternatively, by stabilizing the RF source and/or increasing the modulation frequency. A better mixer could also be used, and, if phase information is not important, heterodyne techniques could be used. An improvement of 20 to 30 dB in sensitivity should permit the smaller flaws of critical size to be detected.

E. Resolution

If radiating antennas are used, the resolution of a microwave NDE system is determined by the wavelength used. Here, resolution is defined as the ability to distinguish between two adjacent flaws in the scanning plane. Because the flaws of interest are smaller than a wavelength, the best resolution obtainable is approximately equal to a wavelength. A lens-focused horn, for example, can provide this maximum resolution. Hence, for an operating frequency of 100 GHz, the resolution is about 3 mm.

The small flaws of interest for ceramic materials might be separated by much less than 3 mm and, hence, would not be resolvable with a 100-GHz

microwave system. On the other hand, high-resolution inspection (when possible) is most practical for small areas. Therefore, microwave NDE may be most suitable for performing rapid inspection of larger areas; inspection of smaller areas could be carried out using other techniques.

F. Scanning Speed

Although, in principle, the noncontacting nature of microwave antennas permits a sample to be scanned rapidly, the scanning rates used during this program were still relatively slow, because they were determined by the available mechanical stage. Typically a 5-inch scan took about one minute; thus, to cover a 5-inch-square area in 0.020-inch steps took about 4 hours.

The maximum permissable scanning speed is approximately equal to the product of the video bandwidth* of the receiver and the characteristic dimension of the smallest flaw that is to be detected. The video bandwidth of the systems used in this program was about 10 Hz; thus, in this case, the maximum scanning rate for 0.5-mm-diameter flaws would be about 5 mm/s, approximately the rate that was used.

One can conclude, therefore, that one must increase the video bandwidth of the receiver to raise the scanning rate. Such widening of bandwidth would be facilitated by increasing the modulation frequency used in the system.

Mechanical scanning arrangements that move the sample in a linear fashion can never achieve high scanning rates because of the relatively large mass that must be moved. This limitation can be overcome by combining rotation of the sample with a linear translation to generate a spiral scan. Alternatively, one could devise methods for scanning the microwave beam, for example, by using a rotating prism or mirror, or by developing a phased-array antenna that can be electronically scanned.

---

*The video bandwidth is assumed to be smaller than the RF bandwidth.

G. Flaw Classification

The cross-polarized C-scan images of seeded defects in Si_3N_4 generated during this program have shown that the differing geometrical shapes of certain types of flaws lead to distinguishable C-scan patterns. For example, iron is distinguishable from silicon, tungsten carbide, and carbon. By combining amplitude information with C-scan patterns, it may also be possible to identify silicon inclusions.

Another potentially useful technique for classifying flaws is to study the variation of microwave scattering with frequency. However, the detection of multiply-scattered waves (such as those generated at the surfaces of the sample) must be suppressed before this technique can be successfully applied in microwave NDE. Also, the system should operate over at least a full waveguide bandwidth, which restricts the microwave components that can be used.

This microwave spectroscopy technique was not evaluated during this program because the microwave systems utilized were both sensitive to multiple scattering, and were narrowband.

H. Quantitative NDE

To provide the necessary information for failure prediction[1] quantitative NDE should be capable of measuring the flaw size and orientation (in 3 dimensions). Now, microwave NDE provides electromagnetic scattering data; there are basically two approaches for utilizing such data to obtain quantitative size information, namely (1) imaging, and (2) inverting the complex amplitude of the scattering. The data taken during this program were all processed to form cross-polarized C-scan images. As discussed in Section V-E, these images possessed the highest resolution obtainable, since focused and near-field antennas were used. However, since the flaws examined were all smaller than a wavelength, their transverse dimensions in the scanning plane could not be accurately determined from the C-scan images. Also, these images do not contain information about the dimensions of the flaws along the direction of propagation of the illuminating wave. Therefore, microwave imaging at

100 GHz cannot provide precise quantitative information on the small flaws of interest in brittle ceramic materials.

To measure the complex amplitude (or magnitude) of the electromagnetic field scattered in specified directions, the microwave system must be calibrated by measuring the scattering from a suitable reference standard over all frequencies and angles of interest. For example, such a standard scatterer could be a sphere, for which the theoretical scattering is known exactly.

In general, the amplitude and phase of the scattered field are functions of:

(1) the frequency

(2) the directions of illumination and observation

(3) the dimensions of the scatterer

(4) the constitutive properties of the scatterer (dielectric constant, conductivity, etc.) and

(5) the spatial characteristics of the illuminating wave.

Therefore, at least as many measurements as independent variables must be made if, say, the dimensions of the scatterer are to be extracted from the data. For this process to succeed, one must also have an accurate inverse-scattering theory for the flaw of interest and precisely measured data (free of multiple scattering) with high signal-to-noise ratio.

All of these requirements seem achievable in principle, but are difficult to achieve in practice with the present state of the art. An alternative approach that may provide some quantitative information would be to develop a statistical data base using characterized flaws in a fixed size and shape of test piece, and then to use these data with computerized adaptive learning techniques[20] for estimating the sizes and shapes of unknown flaws.

I. Reliability and Cost

The reliability of a microwave NDE system is determined primarily by the reliability of the microwave source. Sources that produce high microwave (millimeter-wave) frequencies like 100 GHz are generally

fragile, both electrically and mechanically. However, the predicted lifetime of the more recently developed solid-state sources such as an IMPATT diode typically exceeds 10,000 hours, provided that a well-regulated power supply, adequate temperature control, and cautious turn-on and -off procedures are used. Conventional electron-beam-based sources such as backward-wave tubes, reflex klystrons, etc., can be expected to exhibit lifetimes that are an order of magnitude smaller.

One other microwave component that should be treated with caution is the detector or mixer in the receiver. Because the diodes in this component can be damaged by inadvertant application of a static voltage, an open-circuited cable, for example, should always be discharged before it is connected to such a component.

All other passive 100-GHz components are inherently rugged because of their waveguide-based construction. Therefore, once assembled into a system, they should be highly reliable. One exception, however, is the antenna, whose operation can be degraded by dirty or corrosive environments. For example, no dirt should be allowed to enter an open-ended waveguide or accumulate on the surface of a lens.

The reliability of the nonmicrowave part of the system should be typical of mechanical stages, electronic amplifiers, CRT displays, etc.

The cost of 100-GHZ components has been reduced significantly in the last few years, although some may consider it still rather high. Of course, the cost-effectiveness of a microwave NDE system will be determined by the benefits that are derived in a particular application.

Typical retail costs of 100-GHz components are indicated in Table 2. The most expensive microwave component in a system is usually the RF source. The relatively high cost of the passive components reflects the labor intensiveness and precision required in their fabrication. The total cost of the 100-GHz homodyne system used in this study was about $22,000, and the microwave part of the simpler transmission system cost about $13,000.

Table 2

TYPICAL COSTS FOR 100-GHz MICROWAVE COMPONENTS

IMPATT oscillator with integral isolator and regulated power supply	$ 4,600
Lens-focused Horn	$ 2,000
Ferrite Modulator	$ 1,700
Ferrite Isolator	$ 1,400
Orthomode Coupler	$ 1,100
Directional Coupler	$ 750
Calibrated Attenuator	$ 600
Phase Shifter	$ 500
Rectangular to circular waveguide transition	$ 350
Detector	$ 1,500
Single-ended Mixer	$ 1,700
Straight Length of Waveguide	$ 75
Waveguide Bend or Twist	$ 100
Balanced Mixer-IF Preamplifier	$ 7,000
Phase-Locked IMPATT Oscillator	$10,000
Broadband Backward-wave Sweeping Oscillator	$25,000

At present, because considerable market potential exists for communication and radar systems operating near 100 GHz, one can expect the cost of these components to decrease if this market materializes and if such components are produced in larger quantities.

VI CONCLUSIONS AND RECOMMENDATIONS

The objective of this study has been to determine the best microwave technique or techniques for the NDE of ceramic components and to define the capabilities and limitations of any such technique. The accomplishment of this objective has involved the building of a microwave (100 GHz) measurement system, mechanical X-Y stage, and digital-stage-control and data-acquisition system. Many experiments using seeded Si_3N_4 plates have been performed, and many questions related to practical NDE have been considered. Specific conclusions drawn from this work can be summarized as follows:

- The interior of hot-pressed Si_3N_4 samples up to 1 inch thick can be inspected using 100-GHz electromagnetic waves. SiC exhibits considerably more attenuation than Si_3N_4, but it, too, can be inspected using microwaves if enough RF power is available.
- The usable upper frequency of operation for the microwave NDE of Si_3N_4 is determined by the background clutter associated with surface roughness and grain boundaries or porosity. This clutter begins to be noticeable at 100 GHz for grit-blasted surfaces and reaction-sintered material.
- Using a cross-polarized transmission system with a sensitivity of about -40 dBm and a transmitted power of +5 dBm, one can consistently detect 0.020-inch-diameter inclusions of various types, particularly iron and silicon. In earlier work using a somewhat more sensitive system, smaller inclusions on the order of 0.005 inch in diameter, as well as 0.020-inch-diameter voids, were also detected. Surface cracks 0.050 inch long were not detectable with the sensitivities available, because of their relatively small volumes.
- A local spatial resolution in the scanning plane of about one wavelength (3 mm at 100 GHz) can be achieved.
- The sensitivity of a microwave NDE system is generally determined by the degree to which the coherent clutter generated by specular reflections from the surfaces of the sample can be rejected. The use of mode conversion to reject clutter is moderately successful when the sample is in the form of a plate with plane, parallel faces.
- Mode-conversion techniques will not provide adequate clutter rejection for irregularly shaped samples such as turbine blades.

Inspection of nonplanar samples and achievement of improved sensitivity will require the development of other clutter-rejection techniques such as coherent processing of multiple scans.

- The large amount of microwave scattering caused by a sharp geometrical discontinuity such as an edge generally obscures any small flaws located near such an edge. The local spatial resolution of the system determines how close a flaw can be to an edge and still be detectable by a simple scattering measurement. Inspection to within one to two wavelengths (3 to 6 mm at 100 GHz) from an edge was achieved.
- It appears feasible to classify certain types of flaws (such as iron and silicon) by the shapes of the C-scan scattering patterns they produce. The frequency dependence of the scattering data is another possible classification parameter, but bandwidth limitations in the microwave system and the presence of multiple scattering are problems to be overcome before this parameter can be usefully exploited for classification purposes.
- Quantitative estimation of flaw size and orientation by inverting the scattering data provided by microwave NDE is not currently practical. Also, the resolution provided by 100-GHz C-scan imaging is inadequate for determining the dimensions of the small flaws of interest, but the use of higher frequencies would overcome this problem.
- Microwave NDE systems can be expected to be as reliable as an ultrasonic system, provided that some operator care is exercised, or that automatic circuitry for protecting the RF source and receiver front end is incorporated into the system.
- The present-day cost of a 100-GHz NDE system ($20,000-$40,000) is not unreasonable, particularly if it can provide capabilities not achievable with other NDE techniques. There is also reason to expect that this cost will decrease in the next 5-10 years.

In summary, the work described in this report has provided ample demonstration of the feasibility of microwave cross-polarized scattering for the NDE of Si_3N_4 plates. However, more work is required to improve sensitivity, to adapt the technique to complex geometries, to develop flaw-classification techniques, and to shorten the inspection time. Specifically, areas in need of further study are:

- Clutter rejection--Techniques are needed for improving the rejection of the clutter encountered with planar samples, and also for rejecting the clutter produced by nonplanar samples. The use of a bistatic noncolinear antenna arrangement is one possible approach. Another is the coherent processing of multiple scans that, for example, could be obtained by rotating the sample.

- Improved sensitivity--Techniques for reducing the incoherent system noise such as using a stable source, better mixers, and a higher modulation frequency need to be studied.
- Flaw classification--Given a more sensitive system, flaw-classification techniques using C-scan images and multiple-frequency measurements need further evaluation.
- Beam scanning--The ability to scan the microwave beam and leave the sample fixed should permit inspection times to be reduced. Phased-array and optical beam-scanning techniques should be evaluated for this purpose.

REFERENCES

1. A. G. Evans, et al., "Failure Prediction in Structural Ceramics," Materials Evaluation, Vol. 35, pp. 85-96 (April 1977).

2. R. Kossowsky, "Defect Detection in Hot-Pressed Si_3N_4," Ceramics for High-Performance Applications, J. Burke, A. Gorum, and R. Katz, Eds., pp. 665-685 (Brook Hill Publishing Co., Chestnut Hill, Massachusetts, 1974).

3. D. S. Kupperman, et al., "Preliminary Evaluation of Several Nondestructive-Evaluation Techniques for Silicon Nitride Gas-Turbine Rotors," Argonne National Laboratory Report ANL-77-89, DOE Contract W-31-109-Eng-38 (January 1978).

4. R. Hochschild, "Applications of Microwaves in Nondestructive Testing," Nondestructive Testing, Vol. XXI, pp. 115-120 (March 1963).

5. T. Lavelle, "Microwaves in Nondestructive Testing," Materials Evaluation, Vol. XXV, pp. 254-258 (November 1967).

6. R. J. Botsco, "Nondestructive Testing of Plastics with Microwaves," Materials Evaluation, Vol. XXVII, pp. 25A-32A (June 1969).

7. S. Ramo and J. R. Whinnery, Fields and Waves in Modern Radio, Ch. 7 (John Wiley and Sons, Inc., New York, New York, 1953).

8. P. Barber and C. Yeh, "Scattering of Electromagnetic Waves by Arbitrarily Shaped Dielectric Bodies," App. Opt., Vol. 14, pp. 2864-2872 (December 1975).

9. D. E. Barrick, Radar Cross Section Handbook, G. T. Ruck, Ed., Vol. 1, Ch. 3 (Plenum Press, New York, New York, 1970).

10. A. Hussain and E. A. Ash, "Microwave Scanning Microscopy for Nondestructive Testing," Proceedings of the 5th European Microwave Conference, Hamburg, Germany, pp. 213-217 (September 1975).

11. R. J. Hruby and L. Feinstein, "A Novel Nondestructive, Noncontacting Method of Measuring the Depth of Thin Slits and Cracks in Metals," The Review of Scientific Instruments, Vol. 41, pp. 679-683 (May 1970).

12. U. H. Gysel and L. Feinstein, "Design and Fabrication of Stripline Microwave Surface-Crack Detector for Projectiles," Final Report, Contract DAAG46-73-C-0257, SRI Project 2821, SRI International, Menlo Park, California (September 1974).

13. S. Silver, Ed., "Microwave Antenna Theory and Design," M.I.T. Radiation Lab. Series, Vol. 12, Ch. 11 (McGraw-Hill Book Co., Inc., New York, New York, 1948).

14. P. Wong and D. R. Messier, "Dependence of Mechanical and Dielectric Properties of Si_3N_4 on Fabrication Conditions," Am. Ceram. Soc. Bull. (Abstract), Vol. 52, No. 4, p. 427 (1973).

15. W. B. Weir, "Automatic Measurement of Complex Dielectric Constant and Permeability at Microwave Frequencies," Proc. IEEE, Vol. 62, pp. 33-36 (January 1974).

16. S. Silver, Ed., "Microwave Antenna Theory and Design," M.I.T. Radiation Lab. Series, Vol. 12, Ch. 10 (McGraw-Hill Book Co., Inc., New York, New York, 1948).

17. A. J. Bahr, "Microwave Techniques for Nondestructive Evaluation of Ceramics," Final Report, Contract DAAG46-76-C-0048, SRI Project 5594, SRI International, Menlo Park, California (November 1977).

18. A. G. Evans, "Failure Prediction in Structural Ceramics," paper presented at ARPA/AFML Review of Progress in Quantitative NDE, Scripps Institution of Oceanography, La Jolla, California (July 1978).

19. M. Born and E. Wolf, Principles of Optics, Ch. 13 (Pergamon Press, New York, New York, 1964).

20. A. M. Mucciardi, R. Shankar, J. Cleveland, W. E. Lawrie, and H. L. Reeves, "Adaptive Nonlinear Signal Processing for Characterization of Ultrasonic NDE Waveforms, Task I: Inference of Flat-Bottom Hole Size," AFML-TR-75-24 (1975).

DISTRIBUTION LIST

No. of Copies	To
	Metals and Ceramics Information Center, 505 King Avenue, Columbus, Ohio 43201
1	ATTN: Mr. Harold Mindlin, Director
1	Mr. James Lynch, Assistant Director
12	Commander, Defense Documentation Center, Cameron Station, Building 5, 5010 Duke Street, Alexandria, Virginia 22314
	Office of the Deputy Chief of Staff for Research, Development, and Acquisition, Washington, D.C. 20310
1	ATTN: DAMA-ARZ-E
1	DAMA-CSS
	Commander, Army Research Office, P.O. Box 12211, Research Triangle Park, North Carolina 27709
1	ATTN: Dr. George Mayer
1	Mr. J. J. Murray
	Commander, U.S. Army Materiel Development and Readiness Command, 5001 Eisenhower Avenue, Alexandria, Virginia 22333
1	ATTN: DRCQA-E
1	DRCQA-P
1	DRCDE-D
1	DRCDMD-FT
1	DRCLDC
1	DRCMT
1	DRCMM-M
	Commander, U.S. Army Missile Research and Development Command, Redstone Arsenal, Alabama 35809
2	ATTN: DRDMI-TB, Redstone Scientific Information Center
1	DRDMI-TK, Mr. J. Alley
1	DRDMI-M
1	DRDMI-ET, Mr. Robert O. Black
1	DRDMI-QS, Mr. George L. Stewart, Jr.
1	DRDMI-EAT, Mr. R. Talley
1	DRDMI-QP
	Commander, U.S. Army Troop Support and Aviation Materiel Readiness Command, 4300 Goodfellow Boulevard, St. Louis, Missouri 63120
1	ATTN: DRSTS-PLE(2), Mr. J. Corwin
1	DRSTS-Q
1	DRSTS-M

No. of Copies	To
	Commander, U.S. Army Mobility Equipment Research and Development Command, Fort Belvoir, Virginia 22060
1	ATTN: DRDME-D
1	DRDME-E
1	DRDME-G
1	DRDME-H
1	DRDME-M
1	DRDME-T
1	DRDME-TQ
1	DRDME-V
1	DRDME-ZE
1	DRDME-N
	Commander, U.S. Army Tank-Automotive Materiel Readiness Command, Warren, Michigan 48090
2	ATTN: DRSTA-Q
	Commander, U.S. Army Armament Research and Development Command, Dover, New Jersey 07801
1	ATTN: DRDAR-LC, Mr. E. Kelly
1	DRDAR-LCA, Dr. Sharkoff
1	DRDAR-LCE, Dr. Walker
5	DRDAR-QAS, Mr. F. Fitzsimmons
1	DRDAR-SCM, Mr. J. D. Corrie
1	DRDAR-TSP, Mr. B. Stephans
2	DRDAR-TSS, (STINFO)
	Commander, Watervliet Arsenal, Watervliet, New York 12189
1	ATTN: DRDAR-LCB, Mr. T. Moraczewski
1	SARWV-PPI, Mr. L. Jette
	Commander, U.S. Army Tank-Automotive Research and Development Command, Warren, Michigan 48090
1	ATTN: DRDTA-UL, Technical Library
1	DRDTA-RCKM, Mr. S. Goodman
1	DRDTA-RCKT, Mr. J. Fix
1	DRDTA-RTAS, Mr. S. Catalano
1	DRDTA-TTM, Mr. W. Moncrief
1	DRDTA-JA, Mr. C. Kedzior
	Director, U.S. Army Industrial Base Engineering Activity, Rock Island, Illinois 61299
1	DRXIB-MT, Mr. D. Brim
	Commander, Harry Diamond Laboratories, 2800 Powder Mill Road, Adelphi, Maryland 20783
1	ATTN: DELHD-EDE, Mr. B. F. Willis

No. of Copies	To
	Commander, Aberdeen Proving Ground, Maryland 21005
1	ATTN: STEAP-MT
1	STEAP-TL
1	STEAP-MT-M, Mr. J. A. Feroli
1	STEAP-MT-G, Mr. R. L. Huddleston
	Naval Research Laboratory, Washington, D.C. 20375
1	ATTN: Dr. J. M. Krafft, Code 8430
1	Library, Code 2620
	Air Force Materials Laboratory, Wright-Patterson Air Force Base, Ohio 45433
1	ATTN: AFML-LTM, Mr. W. Wheeler
1	AFML-LLP, Mr. R. Rowand
1	R. W. McClung, Metals and Ceramics Division, Oak Ridge National Laboratory, P.O. Box X, Oak Ridge, Tennessee 37803
	Hughes Aircraft Company, Electron Dynamics Division, 3100 West Lomita Boulevard, Torrance, California 90509
1	ATTN: Dr. Charles A. Escoffery
1	Chief, Materials Engineering Department, Dept. 93-03M, AiResearch Manufacturing Company of Arizona, 402 South 36th Street, P.O. Box 5217, Phoenix, Arizona 85010
	Director, Army Materials and Mechanics Research Center, Watertown, Massachusetts 02172
2	ATTN: DRXMR-PL
1	DRXMR-P
2	DRXMR-M
1	DRXMR-MQ
1	DRXMR-MI, Mr. Darcy
1	DRXMR-L, Dr. Chait
1	DRXMR-AP
2	DRXMR-PR
1	DRXMR-PD
7	DRXMR-MI, Mr. Brockelman